Deposition, accumulation, and alteration of Cl^-, NO_3^-, ClO_4^- and ClO_3^- salts in a hyper-arid polar environment: mass balance and isotopic constraints

Andrew Jackson[1*], Alfonso F. Davila[2], J.K. Böhlke[3], Neil C. Sturchio[4], Ritesh Sevanthi[1], Nubia Estrada[1], Megan Brundrette[1], Denis Lacelle[5], Christopher P. McKay[6], Armen Poghosyan[7], Wayne Pollard[8], Kris Zacny[9]

1. Texas Tech University, Lubbock, TX 79409
2. Carl Sagan Center at the SETI Institute. 189 Bernardo Ave. Mountain View, CA. 94043
3. U.S. Geological Survey, 431 National Center, Reston, VA 20192, USA
4. Department of Geological Sciences, University of Delaware, Newark, DE 19716, USA
5. Department of Geography, University of Ottawa, Ottawa, ON, Canada
6. NASA Ames Research Center, Moffett Field, CA 94035
7. Skolkovo Institute of Science and Technology, Moscow, Russia
8. Department of Geography, McGill University, Montreal, QC, Canada
9. Honeybee Robotics, 398 W Washington Blvd, Suite 200, Pasadena, CA 91103

Abstract

The salt fraction in permafrost soils of the McMurdo Dry Valleys (MDV) of Antarctica can be used as a proxy for cold desert geochemical processes and paleoclimate reconstruction. Previous analyses of the salt fraction in permafrost soils have largely been conducted in coastal regions where permafrost soils are variably affected by aqueous processes and mixed inputs from marine and stratospheric sources. We expand upon this work by evaluating permafrost soils in University Valley, located in the ultraxerous zone where both liquid water transport and marine influences are minimal. We determined the abundances of Cl^-, NO_3^-, ClO_4^- and ClO_3^- in dry and ice-bearing permafrost soils, snow and glacier ice, and also characterized Cl^- and NO_3^- isotopically. The data are not consistent with salt deposition in a sublimation till, nor with nuclear weapon testing fall-out, and instead point to a dominantly stratospheric source and to varying degrees of post depositional transformation depending on the substrate, from minimal alteration in bare soils to significant alteration (photodegradation and/or volatilization) in snow and glacier ice. Ionic abundances in the dry permafrost layer indicate limited vertical transport under the current climate conditions, likely due to percolation of snowmelt. Subtle changes in ClO_4^-/NO_3^- ratios and NO_3^- isotopic composition with depth and location may reflect both transport related fractionation and depositional history. Low molar ratios of ClO_3^-/ClO_4^- in surface soils compared to deposition and other arid systems suggest significant post depositional loss of ClO_3^-, possibly due to reduction by iron minerals, which may have important implications for oxy-chlorine species on Mars. Salt accumulation varies with distance along the valley and apparent accumulation times based on multiple methods range from ~10-30 ky near the glacier to 70-200 ky near the valley mouth. The relatively young age of the salts and relatively low and homogeneous anion concentrations in the ice-bearing permafrost soils point to either a mechanism of recent salt removal, or to relatively modern permafrost soils (< 1 million years). Together, our results show that near surface salts in University Valley serve as an end-member of stratospheric sources not subject to biological processes or extensive remobilization.

1.0 Introduction

The McMurdo Dry Valleys (MDV) of Antarctica are collectively a hyper-arid polar desert environment, but a steep gradient in summer air temperature and water activity exists between the coastal areas and the high elevation valleys (Marchant and Head, 2007). The latter are the

driest, coldest, and oldest in the MDV system (Marchant et al., 2002; Marchant and Head, 2007), and contain various types of ground ice, ranging from pore ice to massive ground ice bodies under a layer of dry regolith of variable thickness (Bockheim, 1995; Bockheim and Hall, 2002; Bockheim, 2007; Bockheim, et al., 2008; Pollard et al., 2012; Lacelle et al., 2011). This upland region does not develop the same pattern of seasonal active layer as observed in coastal Antarctica or in Arctic regions (Marchant and Head, 2007). Furthermore, some studies suggest that the extremely cold climate in the high elevation MDV has dominated for the past 12.5 Ma, and liquid water has played a negligible role in landscape evolution (e.g., Denton et al., 1971, 1984; Sugden et al., 1995; Marchant et al., 1996; 2013; Swanger et al., 2011). However, recent investigations suggest that ice-bearing permafrost might have partially thawed during warmer climate periods in the Quaternary, at least locally (e.g., Dickinson et al., 2012; Lacelle et al., 2013).

Salts in MDV soils and lakes have been extensively studied (e.g. Bockheim, 1979, 1997; Campbell and Claridge, 1977; Toner et al., 2013; Kounaves et al., 2010). The abundance and isotopic composition of anions have been used to evaluate source(s) of anions and their degree and type of post depositional processing, as well as their implications for paleoenvironmental conditions (Bao and Marchant, 2006; Bao et al., 2008; Michalski et al., 2005). Chloride has both direct marine (past flooding events during periods of higher sea level) and atmospheric sources in the lower MDV while Cl^- in the upper MDV is due solely to atmospheric deposition (e.g. Toner et al., 2013). The atmospheric Cl^- component includes both sea-salt chloride (SSC) and secondary atmospheric chloride (SAC) with decreasing SSC content away from the coast (Bao et al., 2008). The soil anion reservoir can include both atmospheric salts deposited directly on the soil surface and older buried salts released by sublimation of buried glacier ice in sublimation tills. NO_3^- is relatively enriched with respect to Cl^- in the upper MDV due to the ultra-xerous conditions that allow it to accumulate in surface soils and decreased marine salt deposition flux (Bockheim, 1997). The isotopic composition of NO_3^- in deposition of snow and glacial ice has been extensively studied, particularly with respect to post depositional processing (e.g. Grannas et al., 2007; Frey et al., 2009). However, the soil isotopic composition of NO_3^- in the MDV has only been surveyed once (Michalski et al., 2005). ClO_4^- has also recently been identified in MDV soils and is generally enriched with respect to NO_3^- compared to less arid systems (Kounaves et

al., 2010; Jackson et al., 2015). Salt reservoirs in MDV soils have been interpreted to contain substantial information about salt sources and post depositional processes that occur in the MDV, and therefore indirectly about paleoclimatic conditions that led to their current abundance and isotopic composition. However, studies that evaluated both the abundances and isotopic compositions of multiple anions concurrently have been limited.

To gain further insights regarding the source(s), deposition, and chemical and hydrologic alterations of salts in cold hyper-arid systems, we investigated the salt fraction in soils from University Valley, a high elevation glacial valley hanging approximately 400 m above the floor of Beacon Valley, in the Quartermain Mountains. An objective of this study was to use the accumulated salts in these soils to evaluate the paleo-environmental conditions responsible for their distribution and isotopic composition. We combined data on the abundance of Cl^-, NO_3^-, ClO_4^- and ClO_3^- in soils, snow and glacial ice, with isotopic measurements of Cl^-, NO_3^-, and ClO_4^-. Our results provide insights regarding the atmospheric deposition of salts and volatile species and their post depositional transformations and transport in soils, snow, and glacial ice. These findings have direct relevance to our understanding of the potential for past episodes of liquid water activity and contribute to a better understanding of the glacial history of the valley. Salt accumulation in University Valley serves as a model of atmospheric salt dynamics in soils not subject to biological processes. These accumulations have potential relevance for the occurrences of NO_3^- (Stern et al. 2015) and ClO_4^- (Hecht et al. 2009) on Mars and the implications for past habitability on that planet, which can be used as a basis for better interpretations of more complex biologically active arid systems.

2.0 Sampling and Methods

2.1 Site Description

The study site is situated in University Valley (77°52'S; 160°45'E; c.a. 2000 m long, 500-700 m wide and 1600-1800 m a.s.l.), a hanging glacial valley perched above Beacon Valley in the Quartermain Mountains (Fig. 1). A small glacier is present at the head of University Valley (henceforth named University Glacier) and a few perennial snow patches occupy small circular depressions, 1-2m deep, on the western side of the valley. Widespread interstitial ground ice occurs as part of the permafrost system beneath a layer of dry soil; the depth to the contact

between this horizon (also known as the ice table) generally increases in a down valley direction (McKay 2009; Marinova et al., 2013). The mean annual air temperature recorded during 2010-2012 was -24°C and at no time does the maximum hourly air temperature rise above 0°C (Lacelle et al., 2013). Based on measured ground temperatures and modeled incoming solar radiation the valley can be divided into two zones based on ground surface temperatures: i) a perennially cryotic zone characterized by ground surface temperatures continuously below 0ºC linked to higher topographic shadowing; and ii) a seasonally non-cryotic zone where ground surface temperatures >0°C occur for up to a few hours on clear summer days (Lacelle et al., 2015).

Surficial sediments consist of a combination of colluvium and talus cones at the base of the valley walls and undifferentiated alpine drifts and an undifferentiated till on the valley floor (Cox *et al*., 2012). The alpine drift is restricted to the upper and central parts of the valley and likely is correlated with the Alpine A and B drifts in adjacent Arena Valley, dated to > 200ka and >1Ma, respectively (Marchant *et al*., 1993). This interpretation fits the optically stimulated luminescence ages obtained from a 95 cm permafrost core in upper University Valley (Lacelle *et al*., 2013). The undifferentiated till, constrained to the lower part of the valley, contains granite erratics and is likely associated with Taylor 4b Drift (>2.7Ma) or an older glaciation (Cox *et al*., 2012).

2.2 Sampling

All soil, ice, snow, and atmospheric deposition samples were obtained during three field seasons (2009, 2010, and 2012). Five vertical soil profiles were collected for geochemical analyses along the main axis of the valley, starting at a distance of 370 m from University Glacier and extending 1980 m down valley (Figure 1). Vertical soil profiles were obtained by digging a trench and sampling its walls, whereas samples of ice-cemented permafrost were obtained using a SIPRE (Snow, Ice and Permafrost Research Establishment) corer. The vertical profile closest to University Glacier (370 m, 2 cm ice table depth) was obtained as a 65 cm long core of ice-cemented permafrost, and two vertical profiles (720 m and 1100 m distance from University Glacier) included a layer of dry soil as well as the underlying ice-cemented permafrost (Figure 1). The vertical profiles obtained at 1200 m and 1940 m from University Valley were composed

146 solely of dry soils and the depth to the ice table was unknown (>40 and >66 cm, respectively). In
147 addition to the profiles, a set of near-surface composite samples of the dry soil layer were
148 collected along a transect from the edge of University Glacier to a distance of 1300 m down
149 valley at 100 m increments. The transect samples (T1-T13) were collected from the surface
150 down to the ice table or to a maximum depth of 20 cm and homogenized prior to subsampling for
151 analysis. In addition, we collected a 1.2 m long core from University Glacier and a 1.0 m core
152 from a perennial snow patch located ~600 m down valley from University Glacier. Samples of
153 fresh snow were also collected during snowfall events in the austral summers of 2010 and 2012.
154 Long-term total atmospheric deposition was collected in a PVC stand pipe (~10 cm diameter and
155 ~1 m above the ground surface) lined with a plastic zip-lock bag. The total atmospheric
156 deposition sampler was deployed in November of 2010 and retrieved in January of 2012. We
157 also evaluated aerosols collected in lower Taylor Valley (2013). Aerosols were sampled by
158 pulling air through filter cartridges containing 25 mm GF/F filters (Whatman 45). The vacuum
159 pump had initial air flow rate of 18 L/min with a filter cartridge attached. Sampling time varied
160 between 3 and 7 days.
161
162 *2.3 Geochemical analyses*
163 Salts in soil samples were extracted in milli-Q water at water:soil ratios between 5:1 and 10:1 by
164 mass. The extracts were centrifuged for 10 minutes, after which the supernatant water was
165 decanted and filtered (0.2 μm). Ice-bearing samples were sliced frozen into ~2 cm sections. Each
166 section was allowed to thaw after which additional milli-Q water was added and the salts
167 extracted as above. The mass of soil was measured after drying at 105°C. Salt concentrations for
168 all soil samples are expressed as mass/mass of dry soil. All analyzed salts had concentrations less
169 than 10 % of saturation values in the aqueous extracts.
170
171 Soil extracts, snow samples, and glacier ice were analyzed for Cl^-, NO_3^- (reported as NO_3-N),
172 ClO_4^-, and ClO_3^- concentrations as described in Jackson et al. (2015). Briefly, ClO_4^- and ClO_3^-
173 were quantified using an ion chromatograph-tandem mass spectrometry technique (IC-MS/MS)
174 that consisted of a GP50 pump, CD25 conductivity detector, AS40 automated sampler and
175 Dionex IonPac AS20 (250 X 2 mm) analytical column. The IC system was coupled with an
176 Applied Biosystems – MDS SCIEX API 2000^{TM} triple quadrupole mass spectrometer equipped

with a Turbo-IonSpray^{TM} source (Rao et al., 2010; Jackson et al., 2015). To overcome matrix effects, all samples were spiked with an oxygen-isotope (^{18}O) labeled ClO_4^- or ClO_3^- internal standard. Chloride and NO_3^- were analyzed following EPA Method 300.0 using a Dionex LC20, an IonPac AS14A column (4 X 250 mm), and an Anion Atlas electrolytic suppressor. Individual sample quantification limits were based on the final dilution of the sample extract. Analytical uncertainty of all anion measurements is less than ±10% of the measured value.

2.4 Stable isotopes

Subsets of the soil, snow, and ice samples were analyzed for NO_3^- stable isotopic composition. $\delta^{15}N$ and $\delta^{18}O$ in NO_3^- were measured by continuous-flow isotope-ratio mass spectrometry on N_2O produced from NO_3^- by bacterial reduction (Sigman et al., 2001; Casciotti et al., 2002; Coplen et al., 2004). The data were calibrated by analyzing NO_3^- isotopic reference materials using published values (Böhlke et al., 2003). For samples with elevated $\Delta^{17}O$ of NO_3^-, $\delta^{15}N$ values determined by the bacterial N_2O method using conventional normalization equations may be slightly higher than the true values (Sigman et al., 2001; Böhlke et al., 2003; Coplen et al., 2004). $\delta^{15}N$ values reported here were not adjusted for this effect because $\Delta^{17}O$ values were not measured in these samples. True $\delta^{15}N$ values were estimated to be approximately 0.7 to 1.6 ‰ lower than reported values, based on analyses of reference materials and reported correlations between $\delta^{18}O$ and $\Delta^{17}O$ of atmospheric NO_3^- in Antarctica and elsewhere (Michalski et al., 2003, 2005; Savarino et al., 2007).

Chlorine isotope ratios in Cl^- were analyzed for a subset of soil, snow, and ice samples. The Cl^- was precipitated as AgCl and converted to CH_3Cl for IRMS analysis of $\delta^{37}Cl$ (Long et al., 1993) at the Environmental Isotope Geochemistry Laboratory, University of Illinois at Chicago. ^{36}Cl abundances in purified Cl^- samples were measured by accelerator mass spectrometry at the Purdue Rare Isotope Measurement Lab (Sharma et al., 2000). Tritium (^3H) concentrations were measured in selected core samples from the permanent snow patch and University Glacier. Samples were prepared by mixing 10 ml of melted snow/ice sample with an equal amount of Ultragold scintillation cocktail. A PerkinElmer Quantulus 1220 liquid scintillation counter was used to measure ^3H concentrations in the samples with a detection limit of 1.0 Bq/L (8 TU).

Stable isotope ratios (Cl and O) and $^{36}Cl/Cl$ ratios were analyzed for one sample of ClO_4^- separated from bulk soil (5-15cm) obtained near the soil profiles collected at 720m and 750m. The bulk soil (~50kg) was leached using DDI water and loaded onto a bi-functional anion-exchange resin (Gu et al., 2011). Details of ClO_4^- extraction, purification, and analysis methods for $\delta^{37}Cl$, $\delta^{18}O$, $\delta^{17}O$, and $^{36}Cl/Cl$ have been described previously (Gu et al., 2011; Hatzinger et al., 2011). Extraction and purification produced $CsClO_4$ salt, which was decomposed to CsCl and O_2. The O_2 was analyzed for oxygen isotope ratios ($\delta^{18}O$ and $\delta^{17}O$) by isotope-ratio mass spectrometry (IRMS). The CsCl was then converted to AgCl and analyzed for $\delta^{37}Cl$ and ^{36}Cl as described above.

2.5 Estimation of salt accumulation times

The total masses of Cl^- and NO_3^- per unit area were estimated from the integrated concentrations down to the maximum depth sampled (Figure 2) using a dry soil bulk density of 1,600 kg/m^3. Concentrations were linearly interpolated between dry soil discrete sample depths. The calculated masses per unit area were then divided by various deposition measurements as described below.

^{36}Cl accumulation times were estimated using the following equation:

$$\text{Accumulation Time} = \sum Cl/Cl_{MW} * 6.023X10^{23} * R_u/D_{36Cl}$$

Where $\sum Cl$ is the total Cl^- mass to a given depth per m^2, $Cl_{MW\ is\ the}$ molecular weight of Cl^-, R_u is the $^{36}Cl/Cl$ ratio of Cl^- in soils in University Valley, and D_{36Cl} is the deposition rate of ^{36}Cl. The ^{36}Cl deposition rate (28,000 atoms/cm^2-year) was based on ^{36}Cl deposition rates in Dome Fuji for 10 kyr B.P. and 22 kyr B.P. (Sasa et al., 2010). The Dome Fuji deposition rates were similar for both time periods evaluated and regardless of the snow accumulation rate, which changed between the LGM and the Holocene by a factor of ~2.4 (Table 1). The Dome Fuji deposition rates match well with other published rates estimated from latitude-dependent modeling (25,000 ±1,600 atoms/cm^2-year) (Synal et al., 1990). The $^{36}Cl/Cl$ ratios of Cl^- in University Valley were fairly constant with depth and between locations, reducing the error imparted by the relatively low number of measured $^{36}Cl/Cl$ ratios.

Total Cl^- accumulation times were estimated using the following equation:

[2] Accumulation Time = $\sum Cl / D_{Cl}$

Where D_{Cl} is equal to the deposition rate of Cl^-. We evaluated three different methods for evaluating D_{Cl}: 1) the maximum and minimum Cl^- deposition rates for low-accumulation glaciers in the MDV, based on snow pits that generally represent deposition since 1948 (Witherow et al., 2006); 2) the measured total Cl^- deposition rate in University Valley measured in this study over a two year period (2010-2012); and 3) the Cl^- deposition rate for Dome Fuji, adjusted for the larger fraction of non-stratospheric (e.g., marine) Cl^- deposition at University Valley, based on the apparent dilution of $^{36}Cl/Cl$ ratios The adjusted Dome Fuji deposition rate ($D_{Cl\text{-}FA}$) that was calculated using the following equation:

[3] $D_{Cl\text{-}FA} = D_{Cl\text{-}F} * R_f / R_u$

where $D_{Cl\text{-}F}$ is equal to the Cl^- deposition rate measured at Dome Fuji, and R_u and R_f are the $^{36}Cl/Cl$ ratios of Cl^- at Dome Fuji and University Valley, respectively.

NO_3^- accumulation times were estimated using a modified version of Equation 2. NO_3^- deposition rates (Table 2) were based on the following reported or measured values: 1) the range reported for low-accumulation MDV glaciers (Witherow et al., 2006); 2) the relation between snow and NO_3^- accumulation developed by Traversi et al. (2012) assuming dry deposition only (no contribution from snow), and a maximum snow deposition rate of 10 cm/year, which should serve as an upper bound given the limited snow fall in Upper MDV valleys (Fountain et al., 1999); and 3) measured total NO_3^- deposition in University Valley (2010-2012) from this study.

3.0 Results

3.1 Concentration and distribution of Cl^-, NO_3^-, ClO_4^- and ClO_3^- salts

Chloride and NO_3^- concentrations ranged between 10 and 1,000 mg/kg of dry soil mass, whereas ClO_4^- and ClO_3^- concentrations were in the µg/kg range. In all vertical dry soil profiles, anion concentrations generally peaked between 5 and 15 cm depth and then decreased downward toward the ice table (where present) (Figure 2). Concentrations of all soluble ions decreased by a factor of ~2 immediately below the ice table and remained constant with depth within the ice-cemented permafrost. Concentrations varied between vertical soil profiles by a factor of 2 to 4, even at decameter scales. NO_3^- was significantly correlated with ClO_4^- ($p<0.05$) in all depth

profiles. Cl^- was significantly correlated with NO_3^- and ClO_4^-, except in the profile at 1200 m (Jackson et al., 2015). Soluble ion concentrations in glacier ice and perennial snow were comparable to those in fresh snow, approximately 1000 times lower than in soils, and relatively constant with depth, except in the case of ClO_3^-, which was more variable (Figure 3).

In general, the total mass of Cl^-, NO_3^-, and ClO_4^- salts per unit area increased with distance from University Glacier for any given depth sampled (Figure 4A, B and Table 1 and 2). Dry soils contained the majority (>70%) of the total mass of anions, with the exception of the profile closest to University Glacier that was composed entirely of ice-cemented sediment. The rate of mass increase with distance from University Glacier was nearly constant for Cl^- and NO_3^-, while the rate of mass increase for ClO_4^- decreased with distance down valley (Figure 4B).

3.2 Variations in ratios of measured anions with respect to location and deposition.

NO_3^-/Cl^- and NO_3^-/ClO_4^- ratios decreased with depth in the dry soils by 40-60% compared to the peak ratio at the concentration maximum at or near the surface (Figure 5 and S1) but were constant with depth in the underlying ice-bearing soil. No such trends with depth were observed for Cl^-/ClO_4^- in dry soils. NO_3^-/ClO_4^- and Cl^-/ClO_4^- but not NO_3/Cl ratios increased with distance from University Glacier (Figure 6). Molar ratios (NO_3^-/ClO_4^-, NO_3^-/Cl^-, Cl^-/ClO_4^-, and ClO_3^-/ClO_4^-) in fresh snow were higher than in total deposition or in aerosols suggesting enrichment of ClO_4^- in dry deposition compared to wet deposition, which is supported by the enrichment in ClO_4^- of aerosols. NO_3^-/ClO_4^- and Cl^-/ClO_4^- ratios of glacier ice and snow pack were generally higher than in total deposition and highly variable exceeding the upper range of fresh snow and total variation in dry soil and ice-bearing soil (Figure 6). NO_3^-/ClO_4^- and Cl^-/ClO_4^- ratios in ice bearing soil were bracketed by ratios in fresh snow. Cl^-/ClO_4^- ratios in dry soils were also bracketed by values in fresh snow but NO_3^-/ClO_4^- ratios in dry soil generally exceeded those in fresh snow. NO_3^-/Cl^- ratios in fresh snow were lower than in total deposition but generally encompassed most soil, snow pack, and glacier ice ratios. Lowest NO_3^-/Cl^- ratios were in glacier ice and snow pack and highest ratios in dry soil. ClO_3^-/ClO_4^- ratios in dry soils and ice-bearing soils were highly variable but consistently lower than all deposition types, snow packs or glacier ice.

3.3 NO_3^- isotopic composition

297 $\delta^{15}N$ and $\delta^{18}O$ values of NO_3^- (NO_3-$\delta^{15}N$ and NO_3-$\delta^{18}O$) in dry soils, ice-cemented permafrost
298 soils, glacier ice and perennial snow patches were within the range of values reported previously
299 for various NO_3^- occurrences in Antarctica (Figure 7). Our $\delta^{18}O$ values (+76 to +84 ‰)
300 overlapped with, but were generally more positive than those reported for other MDV soils
301 (Beacon, Wright, Arena, Mt. Fleming), whereas $\delta^{15}N$ values were similar to those reported for
302 other MDV soils (Michalski et al., 2005). Snow pack and glacier ice had similar NO_3^- isotopic
303 compositions, and both had lower $\delta^{18}O$ values and higher $\delta^{15}N$ values than soils (Figure 7). Fresh
304 snow and total deposition had $\delta^{15}N$ values similar to soils but lower than perennial snow and
305 glacier ice, and $\delta^{18}O$ values higher than snow pack and glacier ice but lower than soils.
306 Compared with previously reported snow values from a traverse on the Polar plateau between
307 Dome C and Dumont d'Urville stations (Frey et al., 2009), soils from University Valley had
308 relatively low $\delta^{15}N$ values and high $\delta^{18}O$ values that were most similar to snow samples collected
309 near the coast. The NO_3^- isotopic composition in the dry soil was comparable to aerosols from
310 Dome C and Dumont d'Urville, and near the seasonal mass-averaged aerosol values for Dumont
311 d'Urville (Savarino et al., 2007, Frey et al., 2009).
312
313 There were small but systematic variations in NO_3-$\delta^{15}N$ and NO_3-$\delta^{18}O$ within and between
314 vertical soil profiles (Figure 7, inset). Within each soil profile, NO_3-$\delta^{15}N$ and NO_3-$\delta^{18}O$ values
315 were significantly positively correlated ($p<0.05$) and slopes were similar for 3 of the 5 profiles
316 (Table S1). In contrast, NO_3-$\delta^{15}N$ and NO_3-$\delta^{18}O$ values of transect soil samples were
317 significantly inversely correlated. In soil profiles, NO_3-$\delta^{15}N$ and NO_3-$\delta^{18}O$ generally decreased
318 with depth, although the overall change in magnitude was small (<2 ‰) (Figure 8). The highest
319 NO_3-$\delta^{15}N$ and NO_3-$\delta^{18}O$ values generally coincided with the peak concentration of NO_3^- in dry
320 soil at or near the ground surface. Isotopic trends in the ice-bearing soils were more variable
321 between profiles. In one profile (750 m) NO_3-$\delta^{18}O$ values decreased with depth below the ice
322 table, while NO_3-$\delta^{15}N$ reached a minimum value at ice table. In another profile (1100 m) NO_3-
323 $\delta^{18}O$ values were relatively constant below the ice table, while NO_3-$\delta^{15}N$ showed an increase (~1
324 ‰ within 1 cm) at the ice table, and decreased with depth .
325
326 There was a strong correlation between NO_3-$\delta^{18}O$ and NO_3-$\delta^{15}N$ values in dry soils and distance
327 down valley from University Glacier ($p=0.005$ for NO_3-$\delta^{18}O$ and <0.001 for NO_3-$\delta^{15}N$) (Figure 6

328 and Table S1). The correlation was positive in the case of NO_3-$\delta^{18}O$ and negative in the case of
329 NO_3-$\delta^{15}N$. Spatial variations in average NO_3-$\delta^{18}O$ and NO_3-$\delta^{15}N$ values between soil profiles
330 were approximately 5 ‰ and 4 ‰, respectively; these were larger than the variations with depth
331 in each profile. Variations of NO_3^- stable isotopic composition in dry soils generally were
332 directly related to measures of NO_3^- abundance (Figure 9 and Table S1). NO_3-$\delta^{18}O$ values within
333 soil profiles, transect samples, and for all data were negatively correlated to $1/NO_3$
334 concentrations and to Cl^-/NO_3^- and ClO_4^-/NO_3^- molar ratios. For the profiles there were generally
335 consistent relationships between isotope ratios and each of the indicators of NO_3^- stability;
336 relations with ClO_4^-/NO_3^- ratios were the most consistent. $\delta^{15}N$ values of soil profiles were not as
337 consistently related to NO_3^- concentrations ($1/NO_3$) but generally were significantly negatively
338 correlated to both Cl/NO_3^- and ClO_4^-/NO_3^- molar ratios (Figure 9). It should be noted that while
339 NO_3-$\delta^{15}N$ values of transect samples were significantly correlated to both $1/NO_3^-$ and ClO_4^-/NO_3^-
340 molar ratios, the slopes of these relationships were of opposite sign compared to those of
341 individual profiles, pointing to at least two distinct processes affecting NO_3^- isotope composition
342 in the dry soils (see Discussion). Variations with depth in soil profiles (increasing $\delta^{15}N$ and $\delta^{18}O$
343 with decreasing relative NO_3^- abundance) could be consistent with isotopic fractionation or
344 mixing, whereas spatial variations along the valley floor (increasing $\delta^{18}O$ with decreasing $\delta^{15}N$
345 and relative NO_3^- abundance) may indicate different sources or depositional environments.
346 Finally, perennial snow and glacier ice had similar NO_3^- isotopic compositions, with lower $\delta^{18}O$
347 values and higher $\delta^{15}N$ values than soils (Figure 7). The trend was reversed with respect to fresh
348 snow and total atmospheric deposition, the latter being depleted in $\delta^{15}N$ but enriched in $\delta^{18}O$.
349
350 *3.4 Cl^- isotopic composition*
351 $\delta^{37}Cl$ values of Cl^- (Cl-$\delta^{37}Cl$) in soils ranged from -3.0 ‰ to -1.3 ‰, generally lower than those
352 reported by Bao et al. (2008) for soils throughout the MDV including Beacon Valley. In the dry
353 soil profiles, Cl-$\delta^{37}Cl$ values were generally lowest at the surface and increased by ~1 ‰
354 immediately below the surface and then were constant with depth both in the dry soil and into
355 the underlying ice-cemented permafrost (Figure 10). Only in the profile closest to University
356 Glacier, composed solely of ice-cemented permafrost, did values of Cl-$\delta^{37}Cl$ decrease with depth
357 (by <1 ‰ over 60 cm). Cl-$\delta^{37}Cl$ values in soil samples were lower by ~1-2 ‰ than in the snow
358 pack or glacier ice.

The $^{36}Cl/Cl$ ratios of Cl^- in soils from University Valley (1800 x 10^{-15} to 2400 x10^{-15}) were higher than those reported for other MDV soils (400 x 10^{-15} to 1200 x 10^{-15}), but lower than those in Dome Fuji ice (~4500 x 10^{-15}) deposited 10-22 kyr ago (Figure 10) (Carlson et al., 1990; Lyons et al., 1998; Sasa et al., 2010). The $^{36}Cl/Cl$ ratios in soil profiles were approximately constant with depth, although two surface samples had the highest measured ratios (~2400 x 10^{-15}). $^{36}Cl/Cl$ ratios in glacier ice and perennial snow (composite samples between 0-125 cm) were 880 x 10^{-15} and 510 x10^{-15}, respectively, and much lower than those in soils, but were similar to values (123 x 10^{-15} to 592 x 10^{-15}) in fresh snow from Taylor Dome (Lyons et al., 1998). Perennial snow patch samples contained both pre- and post-bomb deposition, as indicated by a measurable ^3H peak (23 TU) at a depth of 45 cm, whereas glacier ice appeared to be mainly pre-bomb, as there was no detectable ^3H (<8 TU) (Figure S2). The similarity of $^{36}Cl/Cl$ ratios in pre- and post-bomb deposition snow and ice, combined with the large Cl^- mass/area in soils compared to deposition rates, suggests little or no influence of bomb ^{36}Cl in these soil profiles. The relatively low $^{36}Cl^-/Cl^-$ ratios and relatively high $\delta^{37}Cl$ values in ice and snow samples, compared to those in soil samples, may indicate a larger fraction of sea salt Cl in snow and ice (see Discussion).

3.5 Salt accumulation times

Maximum accumulation times for Cl^- in the dry soil for a constant depth (56cm) at each location varied by a factor of ~ 3 depending on the method used to calculate Cl^- deposition rates (Table 1). The accumulation times increased with distance from the glacier (9,400- 33,500 years near the glacier to 68,000-218,000 years furthest from the glacier). Accumulation times based on ^{36}Cl deposition rates increased with distance from the glacier and ranged from 10,000-71,000 years. Accumulation times for NO_3^- had a similar overall pattern, but were generally greater by a factor of 2-4 (Table 2). The lowest accumulation times based on NO_3^- were calculated using the short-term total NO_3^- deposition rate in University Valley measured in the current study. Other NO_3^- deposition rates were all based on deposition rates measured for snow and glacier ice.

4.0 Discussion

The undifferentiated alpine drift in University Valley consists of ice-cemented permafrost soils overlain by a layer of dry soil whose thickness tends to increase toward the mouth of the valley

(McKay, 2009; Marinova et al., 2013). The soluble salt fraction in both horizons was dominated by Cl^- and NO_3^- (SO_4^{2-} is not discussed in this paper), but there was a marked difference in salt distribution and abundance between the dry soils and the ice-cemented sediments. To better characterize these differences, each of those horizons is discussed separately below.

4.1 Salts in the dry soils: modern atmospheric sources, post-depositional transformations and transport

Salt concentrations in the dry soils are higher than in the ice-bearing permafrost, and more variable with depth and with distance from University Glacier. Total salt concentration in this layer is generally lower than in the low elevation valleys of the MDV, or in Beacon Valley, particularly for deeper soil horizons (Bao et al., 2008; Kounaves et al., 2010). Salt concentrations generally peak at a depth of 10-15 cm, which likely reflects the maximum depth of snowmelt percolation during clear summer days following the accumulation of a thin snow cover, as was visually observed (Figure 2).

In contrast to total salt concentrations, NO_3^- and ClO_4^- concentrations and NO_3^-/Cl^- ratios in the dry soils are generally higher than in the lower MDV and similar to Beacon Valley (Kounaves et al., 2010; Bockheim et al. 1997). ClO_4^- concentrations in University Valley soils are 10 to 100 times higher than in soils from other arid regions on earth, excluding areas with high-grade surface NO_3^- deposits (e.g. Atacama Desert, Mojave Clay Hills, and Turpan Hami) (Jackson et al., 2015). NO_3^-/ClO_4^- molar ratios are lower than in all other known ClO_4^- occurrences except for the Atacama (~10 times lower) and Turpan Hami (similar). Our data support the contention that low NO_3^-/ClO_4^- ratios are due to preservation of atmospheric deposition and lack of input from biological NO_3^- production as proposed by Jackson et al., (2015).

ClO_4^- separated from a single dry soil sample had a $\delta^{18}O$ value of -4.9 ‰ and a $\Delta^{17}O$ value of +12.8 ‰. These are roughly within the range of values reported for ClO_4^- from the Atacama and Mojave Death Valley NO_3^- deposits, although the University Valley $\Delta^{17}O$ value was slightly elevated (by 2-3 ‰) compared to those of any other ClO_4^- samples with similar $\delta^{18}O$ values (Jackson et al., 2010). In contrast, the $\delta^{37}Cl$ value of University Valley ClO_4^- (+1.3 ‰) was similar to those of many other indigenous natural ClO_4^- occurrences, but significantly higher

421 those of Atacama ClO_4^-, and the $^{36}Cl/Cl$ ratio (33,000 x 10^{-15}) was among the highest reported for
422 ClO_4^- in soils and caliches from any location. The strong correlation between Cl^-, NO_3^- and ClO_4^-
423 concentrations, along with the elevated NO_3^-/Cl^- molar ratios and the isotopic compositions of
424 Cl^-, NO_3^-, and ClO_4^- are consistent with atmospheric (possibly stratospheric) sources, limited
425 post depositional transport, and scarce biological activity, as suggested previously for these ions
426 in other MDV soils (Michalski et al., 2005; Savarino et al., 2007; Kounaves et al., 2010; Jackson
427 et al., 2015).
428
429 ClO_3^- has not previously been reported for soils from Antarctica, although it is present in the
430 MDV lakes and other surface waters (Jackson et al., 2012). ClO_3^-/ClO_4^- ratios in University
431 Valley dry soils were less than 1 and commonly were of the order of 0.1, in contrast to other
432 terrestrial arid soils, Mars meteorites, asteroidal meteorites, and lunar samples, for which ClO_3^-
433 $/ClO_4^-$ ratios of the order of 1 or higher have been reported (Rao et al., 2010; Kounaves et al.,
434 2014; Jackson et al., 2015). Lower ClO_3^-/ClO_4^- ratios in soils compared to those in fresh snow,
435 total deposition, aerosols, glacier ice, and perennial snow suggest that soil ClO_3^- may have been
436 subjected to abiotic post-depositional transformations. Partial ClO_3^- loss from soils may have
437 occurred by a mechanism similar to iron-mediated reduction of NO_3^- in MDV ponds and lakes
438 (Samarkin et al., 2010; Murray et al., 2012) but taking place on soil particles, perhaps in thin
439 aqueous films. Alternatively, photochemical oxidation of ClO_3^- to ClO_4^- may have occurred.
440
441 The negative $\delta^{37}Cl$ values and elevated $^{36}Cl/Cl$ ratios of Cl^- in the dry soils indicate that salt input
442 was largely from atmospheric deposition and may have had a substantial (~50%) stratospheric
443 component. Bao et al. (2008) proposed a model in which MDV soil Cl^- is dominated by sea salt
444 chloride (SSC) in valleys near the coast and by secondary aerosol chlorides (SAC) at locations
445 far from the coast, and that sublimation tills should have increasingly negative $\delta^{37}Cl$ values with
446 depth due to the contribution of buried glacial ice. The buried glacial ice, whose origin was
447 attributed to windblown polar plateau snow, was assumed to have very negative $\delta^{37}Cl$ value. A
448 two-component mixing model (Figure 11A) reasonably describes the variation in $\delta^{37}Cl$ and
449 $^{36}Cl/Cl$ values, assuming the stratospheric component had end member values of -4 ‰ (based on
450 northern hemisphere precipitation; Koehler and Wassenaar, 2010) and 4500 x 10^{-15} (average
451 value at Dome Fuji), respectively, and the tropospheric component had end member values of 0

452 ‰ and 1 x 10^{-15} (sea water), respectively. Correlations of both $\delta^{37}Cl$ and $^{36}Cl/Cl$ values with
453 inverse Cl^- concentration (Figure 11B,C) further support this two-component mixing model.
454 Glacial ice and snow had higher $\delta^{37}Cl$ values compared to soil values, contrary to past assertions
455 that the glacial ice in the stable upland zone should have the lowest $\delta^{37}Cl$ values as the ice source
456 is windblown snow from the Polar Plateau (Bao et al. 2008). Cl-$\delta^{37}Cl$ values in vertical soil
457 profiles were not increasingly negative with depth, as has been proposed for sublimation tills
458 (Bao et al., 2008). Based on the lack of Cl-$\delta^{37}Cl$ variation with depth and the lower Cl-$\delta^{37}Cl$
459 values in soil than snow or ice, there is no indication from our study that salts were concentrated
460 in the dry soils by sublimation of buried glacial ice, although some such residual components
461 may be present.
462
463 Our data suggest that variations in soil Cl-$\delta^{37}Cl$ and $^{36}Cl/Cl$ may also be related to relative
464 contributions of wet and dry deposition and that wet deposition contains a larger SSC than dry
465 deposition. This could be due to wet deposition having a larger marine component or that
466 snow/ice accumulates less HCl (stratospheric Cl) than non-acid forms of Cl^-. Our $\delta^{37}Cl$ values
467 are generally more negative than those reported for Beacon Valley, which is the same distance
468 from the coast. This may suggest that elevation plays a role in the relative contributions of
469 deposition types and Cl^- sources (e.g., larger wet deposition contribution in Beacon).
470 Alternatively, as suggested by Bao et al. (2008), the relative contributions of SAC and SSC may
471 have changed over time as Beacon Valley has older soil ages. However, for changes in Cl^-
472 deposition type over time to be responsible for the higher reported Cl-$\delta^{37}Cl$ values in Beacon
473 Valley soils, the Cl^- would need to be well mixed (older Cl^- mixing with younger Cl^- at surface)
474 which is not consistent with isotopic variations observed with depth in Beacon Valley (Bao et al.,
475 2008).
476
477 Variations in NO_3^- stable isotopic composition, both with depth and valley location, revealed
478 important clues about processing of deposited NO_3^- by volatilization, transport, and/or
479 photolysis. Importantly, $\delta^{15}N$ and $\delta^{18}O$ values of NO_3^- in dry soil were similar to those of
480 aerosols and total deposition, but significantly different from those in perennial snow and glacier
481 ice. We interpret the NO_3^- stable isotopic composition of perennial snow and glacier ice as
482 evidence of varying degrees of post depositional fractionation due to combinations of photo-

processing, O exchange, and/or volatilization of HNO_3. Previous studies in Antarctica indicate NO_3^- photolysis and partial re-oxidation may be responsible for large increases in $\delta^{15}N$ and moderate decreases in $\delta^{18}O$ of NO_3^- in snow and ice (Frey et al., 2009; Erbland et al., 2013). Our snow and ice data could be considered qualitatively consistent with such effects, but the relative magnitudes of changes in $\delta^{15}N$ (smaller) and $\delta^{18}O$ (larger) appear to be somewhat different. HNO_3 volatilization may cause variable isotope effects depending on relative importance of fractionations associated with aqueous speciation and vapor emission. Theoretical calculations indicate HNO_3 has higher $\delta^{18}O$ and $\delta^{15}N$ than NO_3^- at equilibrium (Frey et al. 2009; Monse et al. 1969). In this case, if $NO_3^- > HNO_3$ in the perennial snow, then $\delta^{18}O$ and $\delta^{15}N$ of HNO_3 would be higher than those of total (HNO_3+NO_3) and emission of HNO_3 could leave behind NO_3^- with relatively low $\delta^{18}O$ and $\delta^{15}N$ and would not be consistent with $\delta^{15}N$ enrichments observed in perennial snow packs. However, if $HNO_3 > NO_3^-$, then the isotopic composition of HNO_3 would be similar to that of (HNO_3+NO_3^-) and isotope effects could be dominated by kinetic effects of HNO_3 emission, which could leave behind HNO_3 with higher $\delta^{18}O$ and $\delta^{15}N$ (Erbland et al., 2013). Further, if conditions in concentrated aqueous films were strongly acidic and HNO_3 was the dominant species, then O exchange could occur between HNO_3 and H_2O with low $\delta^{18}O$, causing $\delta^{18}O$ of HNO_3 to decrease. In this case, volatilization and exchange could conceivably cause $\delta^{15}N$ to increase and $\delta^{18}O$ to decrease in residual HNO_3 in the perennial snow, as was observed. Variation in the perennial snow and glacier ice NO_3^- isotopic composition did not appear to be related to NO_3^- concentration, Cl^-/NO_3^-, ClO_4^-/NO_3^-, or depth. However, the much higher NO_3^-/Cl^- ratios in soil compared to the perennial snow and glacier ice suggest that either the deposition rate and/or capture rate of NO_3^- and Cl^- were different between ice and soil, or NO_3^- was lost from the perennial snow and ice. HCl has a higher vapor pressure than HNO_3 but it also has a much lower dissociation constant.

In contrast to the perennial snow and glacial ice, soil NO_3^- apparently was more resistant to post-deposition processes affecting its relative abundance and isotopic composition. Major differences between these environments include less light penetration in soil (less photolysis) and acid neutralization by reaction with minerals in soil (less photolysis, volatilization, and isotopic exchange). These results indicate NO_3^- retained in the shallow regolith may be a better monitor

513 of the isotopic composition of atmospheric deposition than NO_3^- retained in ice cores in some
514 hyper-arid environments, though this would not be the case where soils were biologically active.
515
516 Apart from major contrasts between relatively well preserved NO_3^- in soils and more altered
517 NO_3^- in perennial snow and glacier ice, our data also indicate at least two separate processes may
518 have interacted to cause minor variations in NO_3^- stable isotopic composition within the soils.
519 First, isotopic variation with distance from University Glacier could be consistent with varying
520 degrees of processing on ephemeral overlying snow and ice prior to incorporation in the soil.
521 McKay (2009) argued that a decrease in snow recurrence with down-valley distance from
522 University Glacier could explain the observed trend in ice-table depth. We assume that NO_3^-
523 deposited directly onto exposed soil would not be subject to volatilization, photolysis, or water
524 exchange, whereas NO_3^- deposited onto overlying snow and ice would be subject to such post
525 depositional processes. Therefore the relative amount of NO_3^- deposited on snow and ice rather
526 than directly on soil and the relative amount of time that NO_3^- spends in the snow and ice before
527 being transported into the soil could determine the bulk NO_3^- isotopic composition in the soil at
528 each location. If soils near University Glacier were covered by snow more often than soils farther
529 down the valley, then accumulated soil NO_3^- nearer the glacier ought to be more affected by
530 photolysis, volatilization, or O exchange because it was less rapidly neutralized and protected
531 from light exposure. Data supporting this conceptual model include changes in NO_3^- stable
532 isotopic composition with respect to location in the valley, the overall inverse relation between
533 $\delta^{18}O$ and $\delta^{15}N$ (transect samples), and the strong overall relations between $\delta^{18}O$, $\delta^{15}N$, and
534 measures of NO_3^- loss (e.g. ClO_4/NO_3 molar ratio and $1/NO_3$) (Figures 6, 7, 9).
535
536 While down-valley trends were evident in the shallow soil samples (Figure 6), the profile data
537 indicate NO_3^- isotopic composition may have been altered further by processes occurring during
538 vertical transport (dissolution, advection, crystallization) and/or mixing with NO_3^- released from
539 underlying ice-cemented sediments by sublimation at the ice table (Figure 8). Observations
540 supporting an impact from crystallization and transport include: 1) decreasing NO_3^-/Cl^- and NO_3^-
541 $/ClO_4^-$ ratios with depth down to the ice table (Figure 5), 2) decreasing $\delta^{18}O$ and $\delta^{15}N$ with depth
542 and simultaneously with NO_3^- relative abundance, as indicated by $1/NO_3^-$, Cl^-/NO_3^-, and ClO_4^-
543 $/NO_3^-$ (Figure 8 and 9), and 3) co-variation of $\delta^{18}O$ and $\delta^{15}N$ within profiles that is consistent

with isotope fractionation effects (Figure 7). These relations are similar to those reported for $\delta^{18}O$ and $\delta^{34}S$ in SO_4^{-2} in MDV soil profiles and attributed to downward migration and crystallization/transport fractionation effects (Amundsen et al., 2012). However, it is also possible that some of the isotopic variation was due to mixing of relatively *new* atmospheric NO_3^- and *old* NO_3^- released from the ice-cemented permafrost. Mixing could be qualitatively consistent with a series of positive $\delta^{15}N$- $\delta^{18}O$ trends between local deep ground ice values and local shallow soil transect values (Figure 7 inset). However, this effect should be relatively minor given 1) the low NO_3^- concentrations (~10X) in ice-cemented permafrost compared to the overlying dry soil; 2) the observation that isotopic values are not always the most positive at the surface but rather at the concentration maximum, nor are they always the least positive at the ice table; and 3) the sharp transition in anion concentration (2X) between the surface of the ice-cemented permafrost soil and the overlying dry soil (~1cm).

4.2 Salt accumulation times

Our results suggest that salts in University Valley permafrost soils are mostly derived from direct atmospheric deposition and not from lateral remobilization or sublimation of tills. Our calculated salt accumulation times to a depth of 56 cm using deposition rates of Cl^-, NO_3^-, and ^{36}Cl (Table 1 and Table 2) consistently increased with distance from the glacier and were generally consistent between calculation methods, although most estimates based on NO_3^- accumulation in glacier or snow packs but not those based on total deposition were higher than all methods based on Cl^-. The lower NO_3^- deposition rates from glacial and snow studies are likely due to NO_3^- greater tendency for post-depositional processing (photo-transformation and volatilization) which is supported by the low NO_3^-/Cl^- ratios in University Valley snow pack and glacial ice, and altered NO_3^- stable isotope composition in snow packs, glacial ice but not soil NO_3^-. Salt accumulation times are consistent with the lack of variation in $^{36}Cl^-/Cl^-$ ratios which would have been only minimally impacted by decay over the last 100K-200K years particularly considering the large mas of Cl^- accumulated near the surface allowing mixing of older and newer Cl^- deposition. It should be noted that we have no information regarding the mass of salts present below our sample depths and so our discussion only pertains to the salts in the upper 56 cm. We also do not eliminate the possibility that the current salt accumulations are partially due to sublimation of

574 ground ice and deflation of soils with concentration due to limited downward migration of salts
575 from transient melt events. While none of our data directly support this interpretation, it does not
576 change the accumulation time required to account for the accumulated salts observed assuming
577 the salts are atmospheric in origin. These estimated accumulation times are subject to various
578 interpretations.

579 One possible explanation for the increasing salt accumulation time with distance from University
580 Glacier could be the differential stability of HCl and HNO_3 in snow and ice compared to bare
581 soils. If current conditions of snow recurrence in University Valley, with more stable and
582 permanent snow cover towards the head of the valley, persisted during the past 100-200 kyrs,
583 then soils near the head of the valley would be expected to be depleted in Cl^- and NO_3^- due to
584 photolysis and volatilization in snow/ice, compared to bare soils towards the mouth of the valley.
585 The result would be a lower accumulated salt mass near University Glacier, resulting in a lower
586 calculated salt accumulation time even though the true salt accumulation times might have been
587 similar throughout the valley.

588 Another possible scenario might be glacier retreat resulting in the progressive
589 deposition/exposure of permafrost soils in an up-valley direction during the past 100-200 kyrs, a
590 timing that roughly coincides with the age of Alpine A drifts in adjacent Arena Valley, dated to >
591 200 ka (Marchant *et al*., 1993). However, there is no conclusive evidence yet of glaciation in
592 University Valley during the Quaternary, or of a significant change in climate regime that would
593 support this scenario.

594 *4.3 Salts in ice-cemented permafrost sediments(or soils)*
595 Contrary to the dry soils, the abundance, distribution, and isotopic composition of soluble anions
596 in the ice-cemented sediments were relatively monotonous throughout the valley and with depth,
597 with the exception of NO_3^- isotopes, which showed some spatial variation (Figure 2, 6, and 8).
598 To our knowledge such distribution of soluble ions in ground ice has not been reported in the
599 literature previously. There are several mechanisms that could explain the relatively low
600 abundance and homogenous distribution of salts in the ice-cemented permafrost; however, our
601 data are inconclusive.
602

603 Commonly, soils with low salt abundances and featureless vertical salt profiles reflect flushing
604 events whereby percolation of surface water dissolves and carries soluble ions towards deeper
605 soil layers. However, under current conditions, liquid water plays a minimal role in landscape
606 evolution in University Valley, and this has likely been the norm throughout the Quaternary, and
607 perhaps longer (Marchant et al., 2013). Relatively warmer and wetter conditions could have
608 occurred during past interglacial periods triggered by orbital changes, but these are unlikely to
609 cause complete thawing and refreezing of the ice-cemented layer. In addition, stable water
610 isotope analyses show that some of the ground ice in University Valley formed from vapor
611 diffusion and freezing (Lacelle et al., 2013), a result that is incompatible with significant vertical
612 liquid water transport in the soil column, at least locally. The low abundance and homogenous
613 distribution of salts could also be due to cryoturbation and soil mixing, but this also requires
614 partial thawing and refreezing of the ground ice, again inconsistent with the stable isotope data.
615 We note also that other morphological features commonly associated to cryoturbation such as
616 frost heave (sorting) or solifluction lobes are absent in University Valley.
617
618 An alternative explanation would be strain induced cycles of ice recrystallization due to daily
619 and seasonal temperature fluctuations. Ice recrystallization can cause chemical impurities (i.e.
620 salts) to concentrate at grain boundaries, possibly resulting in thin briny films with lower
621 freezing points, which can then migrate along the network of grain boundaries and smooth out
622 any initial chemical layering (Fisher, 1987).
623
624 Finally, the low abundance and homogenous distribution of salts in the ice-cemented
625 permafrost could be due to a very fast sedimentation in a scenario of rapid glacier retreat, leading
626 to the deposition of a glacial till across the valley. In that scenario, melting at the snout of the
627 glacier during its retreat could leach salts deposited with the till, and the subsequent formation of
628 ground ice would prevent further salt deposition from the atmosphere. The mass balance of salts
629 in the soil and the ^{36}Cl data suggest that such event would have happened during the last several
630 hundred thousand years. While there is no independent evidence that can support this event,
631 small alpine glaciers in the McMurdo Sound region respond more quickly to climate variations
632 than do the major glaciers fed from the central plateau (Campbell and Claridge, 1987). In the
633 Beacon Valley area there are five recognized advances of the Taylor Glacier from the north and

634 five recognized advances of Alpine-type glaciers (Linkletter et al., 1973), but the timing of these
635 events has not yet been fully constrained. If the distribution and abundance of the salt fraction in
636 permafrost soils in University Valley indeed points to the last period of advance and retreat of
637 University Glacier, then our age estimates would place this event at approximately 150-200 kyr
638 ago.
639
640 The ultimate mechanism responsible for the salt profile in the ice-cemented soils critically
641 depends on whether there has been a net loss of salt in the sampled profile since the formation of
642 the soil layer. A flushing event or the vertical movement of liquid water would result in a salt-
643 rich layer with depth, which might be below the maximum sampling depth. Such a salt-rich layer
644 would be absent in a scenario of fast sediment deposition followed by ice-accumulation, or
645 mixing due to strain induced cycles of ice recrystallization. While we cannot conclusively rule
646 out any of the above scenarios, the explanation of the observed salt profile in the ice-cemented
647 permafrost will likely provide important insights regarding the formation and evolution of
648 ground ice in this extremely cold and dry environment. Current efforts to establish OSL ages
649 along the valley may help to resolve which scenario is correct.
650
651 **5.0 Conclusions**
652 This study used the abundances and spatial distributions of soluble anions and the isotopic
653 compositions of a subset of these anions to evaluate the salt sources and post depositional
654 alterations in a high-elevation cold hyper-arid valley of Antarctica. We demonstrated that Cl^-,
655 NO_3^-, ClO_3^-, and ClO_4^- in this valley were dominated by atmospheric deposition to the soil
656 surface and varying degrees of post depositional transformation and limited vertical transport.
657 Unlike lower-elevation MDV soils there does not appear to be a substantial contribution of salts
658 from periods before the current accumulation period nor has extensive remobilization occurred
659 based on salt profiles and isotopic composition. As such the salts in University Valley soils may
660 be more robust indicators of past climate conditions and deposition sources.
661
662 We propose the large variations in NO_3^- and Cl^- isotopic composition in perennial snow and
663 glacier ice compared to soils reflect enhanced preservation of isotopic composition in soils as
664 well as differences in the proportion of dry and wet deposition. While the $^{36}Cl^-/Cl^-$ ratios and

665 $\delta^{37}Cl^-$ values support previous conclusions that deposition of sea-salt chloride decreases with
666 distance from the coast, our data are not congruent with past interpretations of depth-dependent
667 changes attributed to the presence or absence of sublimation tills. Our data also indicate that
668 elevated $^{36}Cl/Cl$ ratios are not due to nuclear bomb fallout, but rather may be characteristic of the
669 natural deposition (wet or dry) source of Cl^-. Soil NO_3^- isotopic compositions largely reflect
670 unaltered atmospheric deposition and likely represent some of the best preserved atmospheric
671 NO_3^- occurrences on earth. Small but systematic variations in NO_3^- isotopic composition with
672 depth are likely due to downward transport-related fractionation, while changes with respect to
673 location in University Valley are more likely due to changes in the amount and stability of snow
674 cover in the valley that lead to differing degrees of post depositional transformation. We also
675 propose that ratios of NO_3^- to other conserved species, particularly ClO_4^-, appear to be good
676 indicators of NO_3^- loss and therefore of NO_3^- isotopic fractionation and should be considered in
677 other studies in addition to evaluating changes in concentration directly. The isotopic
678 composition of ClO_4^- in University Valley soil appears consistent with a stratospheric source
679 although smaller amounts of surface production cannot be ruled out.
680
681 The abundance and distribution of salts in the ice-cemented sediments, along with the estimated
682 age of salt deposition, point to either a mechanism of recent salt removal (e.g. water leaching), or
683 to the formation of permafrost soils in relatively modern times (< 500 kyr). Hence, this type of
684 study can provide important insights regarding the hydrology and glacial history of this
685 extremely cold and dry environment.
686
687 The occurrence of both ClO_4^- and ClO_3^- in these soils along with the very limited transport,
688 hyper-arid conditions, and cold temperatures, support the use of this valley as a possible Earth
689 analog of Mars processes. SAM data indicate a constant ratio of NO_3^-/ClO_4^- in Martian soil
690 (Stern et al., 2015). The stability of ClO_3^- in these soils is of particular interest as it could suggest
691 that the ratio of ClO_3/ClO_4 in Martian soils may be a predictor of water availability, although
692 further work is required to understand the exact conditions that lead to ClO_3^- loss in University
693 Valley soils.
694
695 **6.0 Acknowledgements**

This work was supported by the Strategic Environmental Research and Development Program (SERDP Project ER-1435) of the U.S. Department of Defense; the U.S. Geological Survey Toxic Substances Hydrology Program, National Research Program, Groundwater Resources Program, and National Water Quality Assessment Program; Antarctic fieldwork was supported by the NASA ASTEP program, in collaboration with the US Antarctic Program within the NSF Office of Polar Programs. Hillary Dugan and Kyle Cronin (UIC) collected the Taylor Valley aerosol samples. Baohua Gu (ORNL) performed the perchlorate purification for isotopic analysis, Linnea Heraty (UIC) performed Cl stable isotope analyses, and Stanley Mroczkowski (USGS) performed O isotope analyses. Any use of trade, product, or firm names is for descriptive purposes only and does not imply endorsement by the U.S. Government.

7.0 References

Amundsen, R., Barnes, J.D., Ewing, S., Heimsath, A., and Chong, G. (2012) The stable isotope composition of halite and sulfate of hyperarid soils and its relation to aqueous transport. *Geochemica et Cosmochemica* Acta., 99:271-286

Bao H., Marchant D. R. (2006) Quantifying sulfate components and their variations in soils of the McMurdo Dry Valleys, Antarctica. *J. Geophys. Res-Atmospheres.* 111: (16301).

Bao H., Barnes J. D., Sharp Z. D. and Marchant D. R. (2008) Two chloride sources in soils of the McMurdo Dry Valleys, Antarctica. *J. Geophys. Res.* 113: (D03301).

Bockheim, J.G., (1979) Relative age and origin of soils in eastern Wright Valley, Antarctica *Soil Sience*. 128:(3) 142-152

Bockheim, J.G., (1997) Properties and Classifications of Cold Desert Soils from Antarctica. *Soil. Sci. Soc. Am. J.*, 61:224-231

Bockheim, J.G., (1995) Permafrost distribution in the southern circum-polar region and its relation to the environment: A review and recommendations for further research. *Permafrost Periglacial Proc*. 6:27-45

Bockheim, J.G., and Hall, K.J. (2002) Permafrost, active-layer dynamics and periglacial environments of continental Antarctica. *South African Journal of Science.,* 98:(1-2) 82-90

Bockheim, J.G., (2007) Soil processes and development rates in the Quartermain Mountains, Upper Taylor Glacier region, Antarctica. *Geogr. Ann*. A., 89:(3) 153–165.

Bockheim J., Prentice M. L., and McLeod M. (2008) Distribution of glacial deposits, soils, and permafrost in Taylor Valley, Antarctica. *Arctic Antarctic Alpine Res*. 40: 279–286.

Böhlke, J.K., Mroczkowski, S.J., and Coplen, T.B. (2003) Oxygen isotopes in nitrate: new reference materials for 18O:17O:16O measurements and observations on nitrate-water equilibration. *Rapid Com. Mass Spec*., 17: 1835-1846.

Campbell, I.B., Claridge, G.G.C.,(1977) Development and significance of polygenetic features in Antarctic soils. *New Zealand Journal of Geology and Geophysics.* 20(5):919-931

Campbell, I.B., and Claridge, G.G.C. (1987). *Antarctica: Soils, Weathering Processes and Environment: Soils, Weathering Processes and Environment*. Amsterdam: Elsevier

745 Carlson C.A., Phillips, F., Elmore, D. and Bentley, H.W.. (1990) Chlorine-36 tracing of salinity
746 sources in the Dry Valles of Victoria Land, Antarctica. *Geochemica Cosmica Act.* 54:311-318.
747
748 Casciotti, K.L., Sigman, D.M., Hastings, M., Böhlke, J.K., and Hilkert, A. (2002) Measurement
749 of the oxygen isotopic composition of nitrate in seawater and freshwater using the denitrifier
750 method. *Anal. Chem*., 74, 4905-4912.
751
752 Coplen, T.B., Böhlke, J.K, and Casciotti, K.L. (2004) Using dual bacterial denitrification to
753 improve $\delta^{15}N$ determinations of nitrates containing mass independent ^{17}O. Rapid Com. Mass
754 Spec., 18, 245-250.

755 Cox, S.C., Turnbull, I.M., Isaac, M.J., Townsend, D.B., Smith, B.L. (2012). Geology of southern
756 Victoria Land Antarctica. Institute of Geological and Nuclear Sciences, 1:250,000 geological
757 map 22. Lower Hutt, New Zealand, GNS Science.

758 Denton, G. H., Armstrong, R. L., and Stuiver, M. (1971) The late Cenozoic glacial history of
759 Antarctica Edited by: Turekian, K. K. Late Cenozoic glacial ages. 267-307, Yale University
760 Press, New Haven
761
762 Denton, G.H., Prentice, M.L., Kellogg, D.E., and Kellog, T.B. (1984) Late Tertiary history of the
763 Antarctic ice-sheet - evidence from the dry valleys. *GEOLOGY*, 12:5, 263-267
764
765 Dickinson, W.W., Schiller, M., Ditchburn, B.G., Graham, I.J., and Zondervan, A., (2012)
766 Meteoric ^{10}Be from Sirius Group suggests high elevation McMurdo Dry Valleys permanently
767 frozen since 6 Ma: *Earth and Planetary Science Letters*, v. 355, p. 13–19,
768 doi:10.1016/j.epsl.2012 .09.003.
769
770 Erbland, J., Vicars, W. C., Savarino, J., Morin, S., Frey, M. M., Frosini, D., Vince, E., and
771 Martins, J. M. F., (2013), Air-snow transfer of nitrate on the East Antarctic Plateau - Part 1:
772 Isotopic evidence for a photolytically driven dynamic equilibrium in summer. *Atmospheric*
773 *Chemistry and Physics,* v. 13(13), p. 6403-6419,
774

775 Fisher, D. A. (1987) Enhanced flow of Wisconsin ice related to solid conductivity through strain
776 history and recrystallization. The Physical Basis Ice Sheet Modelling. Proceedings of the
777 Vancouver Symposium, August 1987). IAHS Publ. no. 170.
778
779 Fountain, A.G., Lewis, K.J., Doran, P.T. (1999) Spatial climatic variation and its control on
780 glacier equilibrium line altitude in Taylor Valley, Antarctica. *Global and Planetary Change*.
781 22:1-10
782

783 Frey, M., Savarino, J., Morin, S., Erbland, J., and Martins, J.M.F.. (2009) Photolysis imprint in
784 the nitrate stable isotope signal in snow and atmosphere of East Antarctica and implications for
785 reactive nitrogen cycling. *Atmospheric Chemistry and Physics.* 9:8681-8696
786
787 Grannas, A. M., Jones, A. E., Dibb, J., Ammann, M., Anastasio, C., Beine, H. J., Bergin, M.,
788 Bottenheim, J., Boxe, C. S., Carver, G., Chen, G., Crawford, J. H., Domine, F., Frey, M. M.,
789 Guzman, M. I., Heard, D. E., Helmig, D., Hoffmann, M. R., Honrath, R. E., Huey, L. G.,
790 Hutterli, M., Jacobi, H. W., Klan, P., Lefer, B., McConnell, J., Plane, J., Sander, R., Savarino, J.,
791 Shepson, P. B., Simpson, W. R., Sodeau, J. R., von Glasow, R., Weller, R., Wolff, E. W., Zhu,
792 T., (2007) An overview of snow photochemistry: evidence, mechanisms and impacts.
793 *Atmospheric Chemistry and Physics.* 7(16):4329-4373
794
795 Gu, B., Böhlke, J.K., Sturchio, N.C., Hatzinger, P.B., Jackson, W.A., Beloso, A.D., Heraty, L.J.,
796 Bian, Y., Jiang, X., and Brown, G.M., 2011, Applications of selective ion exchange for
797 perchlorate removal, recovery, and environmental forensics. in SenGupta, A. K., ed., Ion
798 Exchange and Solvent Extraction: A Series of Advances: 20. Taylor & Francis, p. 117-144.
799
800 Hatzinger, P.B., Böhlke, J.K., Sturchio, N.C., and Gu, B. (2011) Guidance Document:
801 Validation of Chlorine and Oxygen Isotope Ratios to Differentiate Perchlorate Sources and
802 Document Perchlorate Biodegradation. Environmental Security Technology Certification
803 Program. 107 pp. Online: http://www.clu in.org/download/contaminantfocus/perchlorate/
804 Perchlorate-ER-200509-GD.pdf.
805 Hecht, M.H., Kounaves, S.P., Quinn, R.C., West, S.J., Young, S.M.M., Ming, D.W., Catling,
806 D.C., Clark, B.C., Boynton, W. V, Hoffman, J., Deflores, L.P., Gospodinova, K., Kapit, J.,
807 Smith, P.H., 2009. Detection of perchlorate and the soluble chemistry of martian soil at the
808 Phoenix lander site. *Science* 325, 64–67.
809 Jackson, W.A., Davila, A., Estrada, N., Lyons, W.B., Coates, J.D., and Priscu, J. (2012)
810 Perchlorate and chlorate biogeochemistry in ice-covered lakes of the McMurdo Dry Valleys,
811 Antarctica. *Geochemica et Cosmochimica Acta*., 98, pp 19-30.
812
813 Jackson, W.A., Böhlke, J.K., Gu, B., Hatzinger, P.B., and Sturchio, N.C., 2010. Isotopic
814 composition and origin of indigenous natural perchlorate and co-occurring nitrate in the
815 southwestern United States. *Environ. Sci. Technol.* 44, 4869–76. doi:10.1021/es903802j
816
817 Jackson, W.A., J.K. Bohlke, Brian J. Andraski, Lynne Fahlquist, Laura Bexfield, Frank D.
818 Eckardt, John B. Gates, Alfonso F. Davila, Christopher P. McKay, Balaji Rao, Ritesh Sevanthi,
819 Srinath Rajagopalan, Nubia Estrada, Neil Sturchio, Paul B. Hatzinger, Todd A. Anderson, Greta
820 Orris, Julio Betancourt, David Stonestrom, Claudio Latorre, Yanhe Li, Greg Harvey. (2015)

821 Global patterns and environmental controls of perchlorate and nitrate co-occurrence in arid and
822 semi-arid environments. *Geochemica et Cosmica Acta*. 164:501-522.
823 doi:10.1016/j.gca.2015.05.016
824
825 Koehler, G. and Wassenaar, L. (2010) The stable isotopic composition (37Cl/35Cl) of dissolved
826 chloride in rainwater. *Applied Geochemistry*. 25:91-96
827
828 Kounaves, S. P., Carrier, B. L., O'Neil, G. D., Stroble, S. T., and Claire, M. W. (2014) Evidence
829 of martian perchlorate, chlorate, and nitrate in Mars meteorite EETA79001: Implications for
830 oxidants and organics. *Icarus*, v. 229, p. 206-213
831
832 Kounaves S.P., Stroble S.T., Anderson R.M., Moore, Q., Catling D.C., Douglas S., McKay C.P.,
833 Ming D.W., Smith P.H., Tamppari L.K., and Zent A.P. (2010) Discovery of natural perchlorate
834 in the Antarctic Dry Valleys and its global implications. *Environ Sci Technol*, 44, 2360-2364.

835 Lacelle, D., Lapalme, C., Davila, A. F., Pollard, W.H., Marinova, M., Heldmann, J., McKay, C.
836 P. (2015) Solar Radiation and Air and Ground Temperature Relations in the Cold and Hyper-
837 Arid Quartermain Mountains, McMurdo Dry Valleys of Antarctica. *Permafr. Periglac. Process*.
838 doi: 10.1002/ppp.1859

839 Lacelle, D., Davila, A.F., Fisher, D.A., Pollard, W.H., DeWitt, R., Heldmann, J.L., Marinova,
840 M.M., McKay, C.P. (2013). Excess ground ice of condensation-diffusion origin in University
841 Valley, McMurdo Dry Valleys of Antarctica: evidence from isotope geochemistry and numerical
842 modeling. *Geochimica et Cosmochimica Acta* 120, 280-297.
843
844 Lacelle, D. Davila, A., Pollard, W.H., Andersen, D., Heldmann, J., Marinova, M., and McKay,
845 C.P. (2011) Stability of massive ground ice bodies in University Valley, McMurdo Dry Valleys
846 of Antarctica: using stable O-H isotopes as tracers of sublimation in hyper-arid regions. Earth
847 and *Planetary Science Letters* 301, 403-411.
848
849 Linkletter, G., Bockheim, J., and Ugolini, F.C. (1973). Soils and Glacial Deposits in the Beacon
850 Valley, Southern Victoria Land, Antarctica. *New Zealand Journal of Geology and Geophysics*
851 16 (1): 90–108. doi:10.1080/00288306.1973.1042538
852
853 Long, A., Eastoe C.J., Kaufmann, R.S., Martin, J.G., Wirt, L., Finley, J.B. (1993) High-precision
854 measurement of chlorine stable isotope ratios. *Geochimica et Cosmochimica Acta* 57: 2907-2912.
855
856 Lyons, W.B., Welch, K.A., and Sharma, P. (1998) Chlorine-36 in the waters of the McMurdo
857 Dry Valley lakes, southern Victoria Land, Antarctica: Revisited. *Geochimica et Cosmochimica*
858 *Acta* 62:185-19

859 Marchant, D.R, Swisher, C.C., Lux, D.R., West, D.P., Denton, G.H. (1993) Pliocene
860 Paleoclimate and East Antarctic Ice-Sheet History from Surficial Ash Deposits, *Science*.
861 260(5108):667-670

862 Marchant, D.R., Denton, G.H., Swisher, C.C. and Potter, N. (1996) Late Cenozoic Antarctic
863 paleoclimate reconstructed from volcanic ashes in the Dry Valleys region of southern Victoria
864 Land. *Geological Society Of America Bulletin*., 108:2, 181-194
865
866 Marchant, D.R. Lewis, A.R., Phillips, W.M., Moore, E.J., Souchez, R.A., Denton, G.H., Sugden,
867 D.E., Potter, N, and Landis, G.P. (2002). Formation of patterned ground and sublimation till over
868 Miocene glacier ice in Beacon Valley, southern Victoria Land, Antarctica. *Geol. Soc. Am. Bull*.,
869 114, pp.718–730.
870
871 Marchant, D.R.; Head, J.W., (2007) Antarctic dry valleys: Microclimate zonation, variable
872 geomorphic processes, and implications for assessing climate change on Mars. *Icarus*, 192(1),
873 187–222.
874
875 Marchant, D.R. Mackay, S.L., Lamp, J.L., Hayden, A.T., Head, J.W. (2013) A review of
876 geomorphic processes and landforms in the Dry Valleys of southern Victoria Land: implications
877 for evaluating climate change and ice-sheet stability. *Geol. Soc. London, Spec. Publ*., 381(1),
878 319–352.
879
880 Mckay, C. P. (2009) Snow recurrence sets the depth of dry permafrost at high elevations in the
881 McMurdo Dry Valleys of Antarctica. *Antarctic Science*, 21:1, 89-94.
882
883 Marinova, M., McKay, C.P., Pollard, W.H., Heldman, J.L., Davila, A.F., Andersen, D.T.,
884 Jackson, A.W., Lacelle, D., Paulson, G., Zacny, K. (2013) Distribution of depth to ice-ceme nted
885 soils in the high-elevation Quartermain Mountains, Dry Valleys of Antarctica. *Antarctic Science*
886 25, 575-582.
887
888 Michalski, G., Scott, Z., Kabiling, M., Thiemens, M.H., (2003) First measurements and
889 modeling of Delta O-17 in atmospheric nitrate. *Geophysical Research Letters.* 30(16): 1870

890
891 Michalski G., Bockheim J. G., Kendall C. and Thiemens M. (2005) Isotopic composition of
892 Antarctic Dry Valley nitrate:Implications for NO(y) sources and cycling in Antarctica. *Geophys.*
893 *Res. Lett.* 32, 13817.
894
895 Monse, E.U., W. Spindel, and M.J. Stern. (1969) Analysis of Isotope-effect Calculations
896 Illustrated with Exchange Equilibria Among Oxynitrogen Compounds. In Isotope Effects in
897 Chemical Processes, ed. W. Spindel, 148-184. Washington, D. C.: American Chemical Society.

Murray, A.E., Kenig, F., Fritsen, C.H., McKay, C.P., Cawley, K.M., Edwards, R., Kuhn, E., McKnight, D.M., Ostrom, N. E., Peng, V., Ponce, A., Priscu, J.C., Samarkin, V., Townsend, A. T., Wagh, P., Young, S.A., Yung, P.T., Doran, P.T. (2012) Microbial life at -13 degrees C in the brine of an ice-sealed Antarctic lake. *Proceedings of the National Academy of Sciences of the United States of America.* 109(50):20626-20631

Pollard, W.H., Lacelle, D., Davila, A.F., Andersen, D., McKay, C.P., Marinova, M., Heldman, J. (2012) Ground ice conditions in University Valley, McMurdo Dry Valleys, Antarctica. Proceedings Tenth International Conference on Permafrost, volume 1: Edited by K.M. Hinkel, Salekhard, Yamal-Nenets Autonomous District, Russia, June 25–29, 2012, The Northern Publisher, pp. 305-310.

Rao, B., Hatzinger, P., Bohlke, J.K., Sturchio, N., Andraski, B., Eckardt, F., and Jackson, W.A. (2010) Natural Chlorate in the Environment: Application of a new IC-ESI/MS/MS Method with a $Cl^{18}O_3$- Internal Standard. *Environ. Sci. Technol*., 44(22), pp6934-6938

Samarkin V.A., Madigan, M.T., Bowles, M.W., Casciotti, K.L., Priscue, J.C., McKay, C.P., and Joye, S.B.(2010) Abiotic nitrous oxide emission from the hypersaline Don Juan Pond in Antarctica. *Nat Geosci*., 3:341–344.

Sasa, K., Y. Matsushi, Y. Tosaki, M. Tamari, T. Takahashi, Y. Nagashima, K. Horiuchi, H. Matsuzaki, Shibata, Y., Hirabayashi, M., and Motoyama, H.. (2010) *Nuclear Instruments and Methods in Physics Research B*., 268:1193-1196.

Savarino J., Kaiser, J., Morin, S., Sigman, D.M., and Thiemens, M.H.. (2007) Nitrogen and oxygen isotopic constraints on the origin of atmospheric nitrate in coastal Antarctica. *Atmos. Chem. Phys*., 7:1925-1945.

Sharma, P., Bourgeois, M., Elmore, D., Granger, D., Lipschutz, M.E., Ma, X., Miller, T., Mueller, K., Rickey, F., Simms, P., Vogt, S. (2000) PRIME lab AMS performance, upgrades and research applications. *Nuclear Instruments and Methods in Physics Research B.* 172:112–123

Sigman, D.M., Casciotti, K.L., Andreani, M., Barford, C., Galanter, M., and Böhlke, J.K. (2001) A bacterial method for the nitrogen isotopic analysis of nitrate in seawater and freshwater. *Anal. Chem*. 2001, 73, 4145-4153.

Stern, J. C., Sutter, B., McKay, C. P., Navarro-Gonzalez, R., Freissinet, C., Conrad, P. G., Mahaffy, P.R., Archer, P.D., Ming, D.W., Niles, P.B., Zorzano, M.-P., and Martin-Torres, F. J. (2015). The Nitrate/Perchlorate Ratio on Mars as an Indicator for Habitability. In Abstracts of the Lunar and Planetary Science Conference (Vol. 46, p. 2590)

Sugden, D.E., Marchant, D.R., Potter, N., Souchez, R.A.,Denton, G.H., Swicher III, C.C., and Tison, J.L. (1995) Preservation of Miocene Glacier Ice In East Antarctica. *Nature*, 376:6539, 412-414

Swanger, K.M., Marchant, D.R., Schaefer, J.M., Winckler, G., Head, J.W. (2011) Elevated East Antarctic outlet glaciers during warmer-than-present climates in southern Victoria Land *Global and Planetary Change.* 79(1-2) 61-72

Synal, H., Beer, J., Bonani, G., Suter, M., Wolfli, W. (1990) Atmospheric transport of bomb-produced 36Cl. *Nuclear Instruments and Methods in Physics Research*. B52:483-488.

Toner, J.D., Sletten, R.S., Prentice, M.L.(2013) Soluble salt accumulations in Taylor Valley, Antarctica: Implications for paleolakes and Ross Sea Ice Sheet dynamics. *Journal of Geophysical Research-Earth Surface.* 118(1):198-215

Traversi, R., Usoskin, I.G., Solanki, S. K., Becagli, S., Frezzotti, M., Severi, M., Stenni, B., Udisti, R. (2012) Nitrate in Polar Ice: A New Tracer of Solar Variability. *Solar Physics* .280(1):237-254

Witherow, R.A., Lyons, W.B., Bertler, N.A., Welch, K.A., Mayewski, P.A., Sneed, S.B., Nylen, T., Handley, M.J., Fountain, A. (2006) The Aeolian flux of calcium, chloride and nitrate to the McMurdo Dry Valleys landscape: evidence from snow pit analysis. *Antarctic Science*. 18(4):497-505

Table 1. Ranges of Cl^- accumulation time in profiles along University Valley based on Cl^- or $^{36}Cl^-$ deposition rates.

Profile	Distance From Glacier	Total Depth	∑Cl	R_U	R_F	Estimated Ages				
University Valley Measured Values					Sasa et al., 2010			Whitherow et al., 2006 MDV		Measured Total Deposition This Study
				$^{36}Cl/Cl*10^{-15}$ Avg(Stdev)	$^{36}Cl/Cl*10^{-15}$ Avg(Stdev)	D_{36Cl}[1] ^{36}Cl Deposition (28,000±1,600 atoms/cm^2-year)	D_{Cl}[2] Cl Deposition normalized for ^{36}Cl ratio (3.8±0.4 mg/m2-y)*R_F/R_U	D_G[3] Estimated Cl^3 Deposition from Glaciers		D_U[4] University Valley year cumulative Collection)[4]
								2.9 mg/m^2-y	6 mg/m^2-y	2.4 mg/m^2-y 4
	(m)	(cm)	(mg/m^2)	(Atom/Atom)	(Atom/Atom)	Years				
1	170	56	80,470	1,990 (96)	4,512 (789)	9,800	9,400	28,100	13,400	33,500
3	575	56	189,000	1, 920 (56)	4,512 (789)	22,300	21,200	66,100	31,500	79,000
4	951	56	349,000	2,200 (260)	4,512 (789)	47,200	45,000	122,000	58,200	145,000
5	1941	56	525,000	2,200(260)	4,512 (789)	71,000	68,000	184,000	87,500	219,000

1. Age estimated based on the total ^{36}Cl atoms in each profile and the ^{36}Cl deposition rate for Dome Fuji between 10,000 and 22,000 years ago from Sasa et al., 2010. $(\sum Cl * Cl_{MW}*R_u)/D_{36Cl.}$

2. Age estimated based on the total Cl in each profile and the Cl deposition rate estimated form the Dome Fuji deposition rate adjusted for dilution of non-stratospheric Cl based on the ratios of 36Cl at each site. $(\sum Cl / [(Rf/R_u)*D_{Cl}]$.

3. Age estimated based on the total Cl in each profile and the Cl deposition rate reported (Whitherow et al., 2006) for the range of MDV low accumulation glaciers. $(\sum Cl / D_G]$.

4. Age estimated based on the total Cl^- in each profile and the measured total Cl^- deposition rate measured in University Valley from 2010-2012.

Table 2.Ranges of NO_3^- accumulation time in profiles along University Valley based on deposition rates.

Profile	Distance From Glacier	Total Depth	∑NO_3-N	Estimated Ages Based on Various NO_3 Deposition Values				
				MDV Low Accumulation Glaciers (Whitherow et al., 2006))		Snow ITASE Traverse (Traversi et al., 2012)		University Valley Measured Total Deposition This Study
				[a]$D1_{NO3}$ (0.55 mg/cm^2-year)	[a]$D2_{NO3}$ (0.87 mg/cm^2-year)	[a]$D3_{NO3}$ (0.67 mg/m^2-year)	[a]$D4_{NO3}$ (1.1 mg/m^2-year)	[b]$D5_{NO3}$ (3.6 mg/m^2-year)
	(m)	(cm)	(mg/m^2)	Years				
1	170	56	66,000	121,000	76,000	99,000	59,000	18,000
3	575	56	146,000	267,000	168,000	218,000	130,000	41,000
4	951	56	268,000	491,000	309,000	400,000	239,000	74,000
5	1941	56	534,000	978,000	615,000	797,000	477,000	148,000

a. Age estimated based on the total NO_3 in each profile and the deposition rate reported for the range of MDV low accumulation glaciers (Whitherow et al., 2006) or the relationship developed for NO_3 accumulation and snow accumulation assuming either dry deposition only or a maximum snow accumulation rate of 10cm w.e. /year as an upper bound given there is no snow accumulation in University Valley.

b. Age estimated based on the total NO_3 in each profile and the measured total NO_3 deposition rate measured in University Valley from 2010-2012.

Table S1. Statistical relationships (r^2, P values, and slopes) between $\delta^{18}O$ and $\delta^{15}N$ of NO3 with various variables. Note that for Transect samples location in Valley is replaced with depth of sample.

Profile	$\delta^{18}O\text{-}NO_3$ (‰)														
	r^2					Slope					P				
	Cl/NO3	1/NO3	NO3/ClO4	Depth/ Location*	$\delta^{18}O\text{-}NO_3$	Cl/NO3	1/NO3	NO3/ClO4	Depth/ Location*	$\delta^{18}O\text{-}NO_3$	Cl/NO3	1/NO3	NO3/ClO4	Depth/ Location*	$\delta^{18}O\text{-}NO_3$
(m)	(mol/mol)	(kg/mg)	(mol/mol)	(‰/cm) or (‰/m)*	‰/‰	(‰*mol/mol)	(‰*mg/kg)	(‰*mol/mol)	(‰/cm) or (‰/m)*	‰/‰	(mol/mol)	(kg/mg)	(mol/mol)	(‰/cm) or (‰/m)	‰/‰
720	0.87	0.90	0.23	0.62		-6.7	-420	-26,000	-.065		0.008	<.001	0.22	0.02	
750	0.45	0.30	0.51	0.66		-3.1	-208	-23,000	-.032		0.14	0.256	0.11	<.001	
1000	0.91	0.76	0.77	0.42		-4.3	-190	-51,000	-.017		0.03	0.05	0.05	0.24	
1100	0.93	0.57	0.93	0.57		-3.6	-297	-31,000	-.041		<.001	0.012	<.001	0.001	
1980	0.92	0.62	0.8	0.22		-3.2	-420	-33,000	-.017		0.001	0.02	0.003	0.24	
Transect	0.003	0.60	0.9	0.5*		0.8	-350	-57,000	-.003*		0.84	0.001	<.001	0.004*	
All	0.28	0.30	0.76	0.4*		-2.4	-180	-46,000	-.003*		0.05	<.001	<.001	0.005*	
	$\delta^{15}N\text{-}NO_3$														
720	0.92	0.22	0.7	0.87	0.55	-2.1	-99	-18,000	-.030	0.37	0.008	0.13	0.009	<.001	0.09
750	0.67	0.53	073	0.48	0.02	-2.4	-26	-8,600	-.0084	0.04	0.015	0.005	<.001	0.008	0.72
1000	0.99	0.71	0.92	0.84	0.78	-3.0	-120	-35,000	-.016	0.57	<.001	0.07	0.01	0.028	0.047
1100	0.95	0.09	0.43	0.51	0.88	-3.2	-39	-17,000	-.035	0.82	<.001	0.19	0.001	0.003	<.001
1980	0.78	0.50	0.50	0.27	0.87	-2.5	-350	-24,000	-.018	0.86	0.021	0.05	0.05	0.19	<.001
Transect	0.21	0.3	0.53	0.63	0.63	-9.5	400	70,000	-.006	-1.3	0.10	0.04	0.003	<.001	<.001
All	0.35	0.04	0.03	0.56		-7.6	87	-12,000	-.005		<.001	0.10	0.16	<.001	

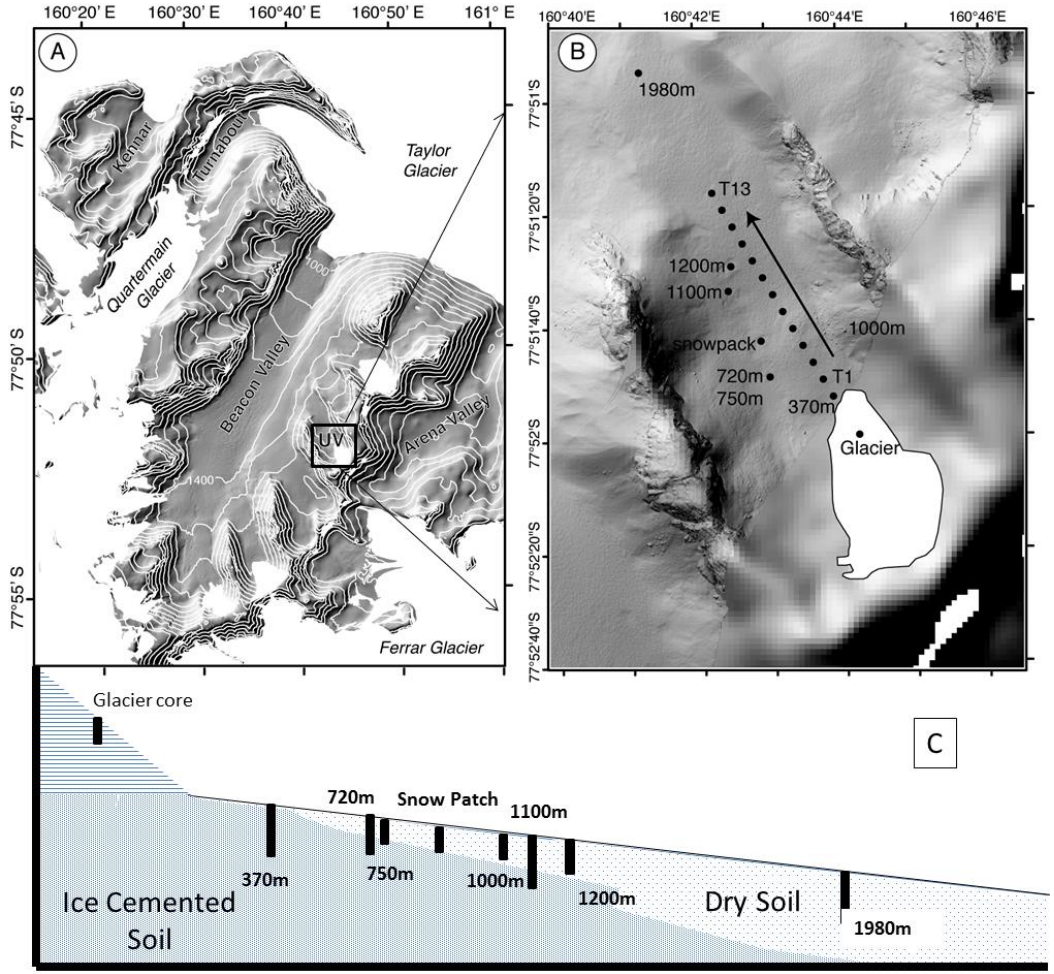

Figure 1. A) Location of University Valley relative to Beacon Valley within the MDV; B) Location of soil profiles with University Valley; and C) a conceptual cross section of University Valley.

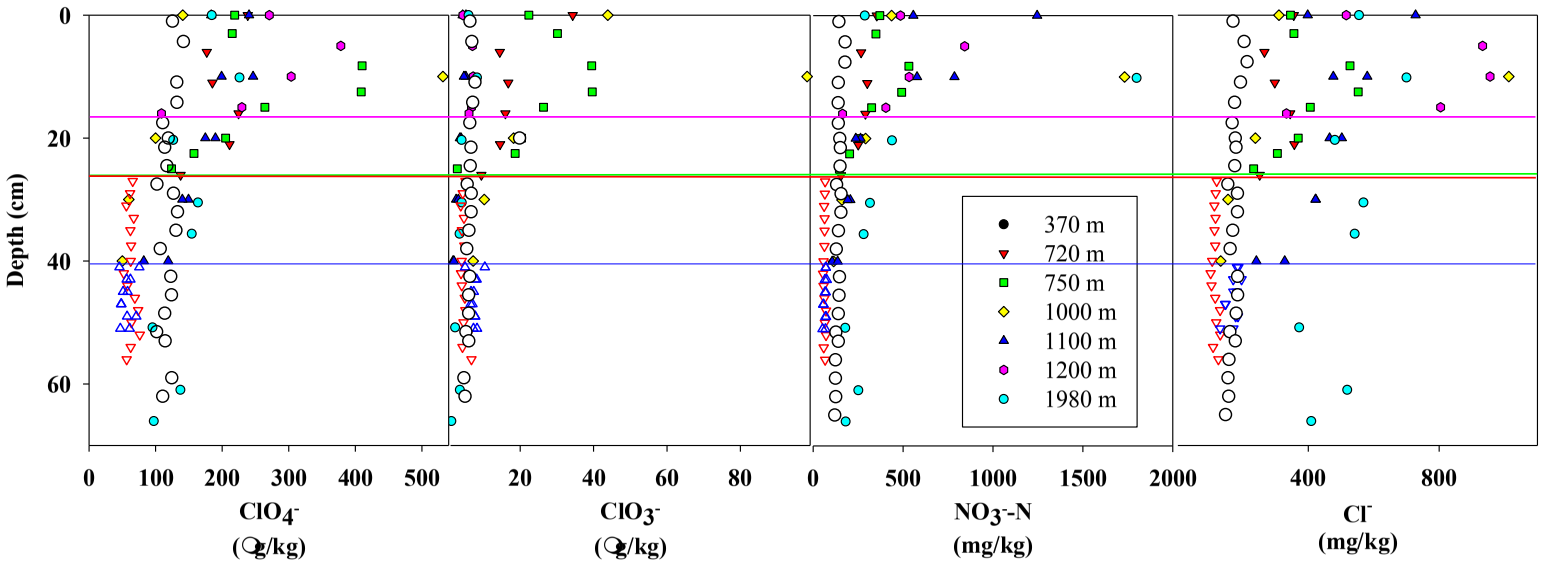

Figure 2- Depth profiles of anion concentrations in University Valley soils at various distances downgradient from University Glacier. Filled symbols indicate values in dry cryotic soil and open symbols indicate values in ice-cemented soil. Horizontal lines indicate the depth to the top of ice-cemented soil (ice table). All concentrations are given in units of mass per kg of dry soil equivalent (i.e., after removal of water).

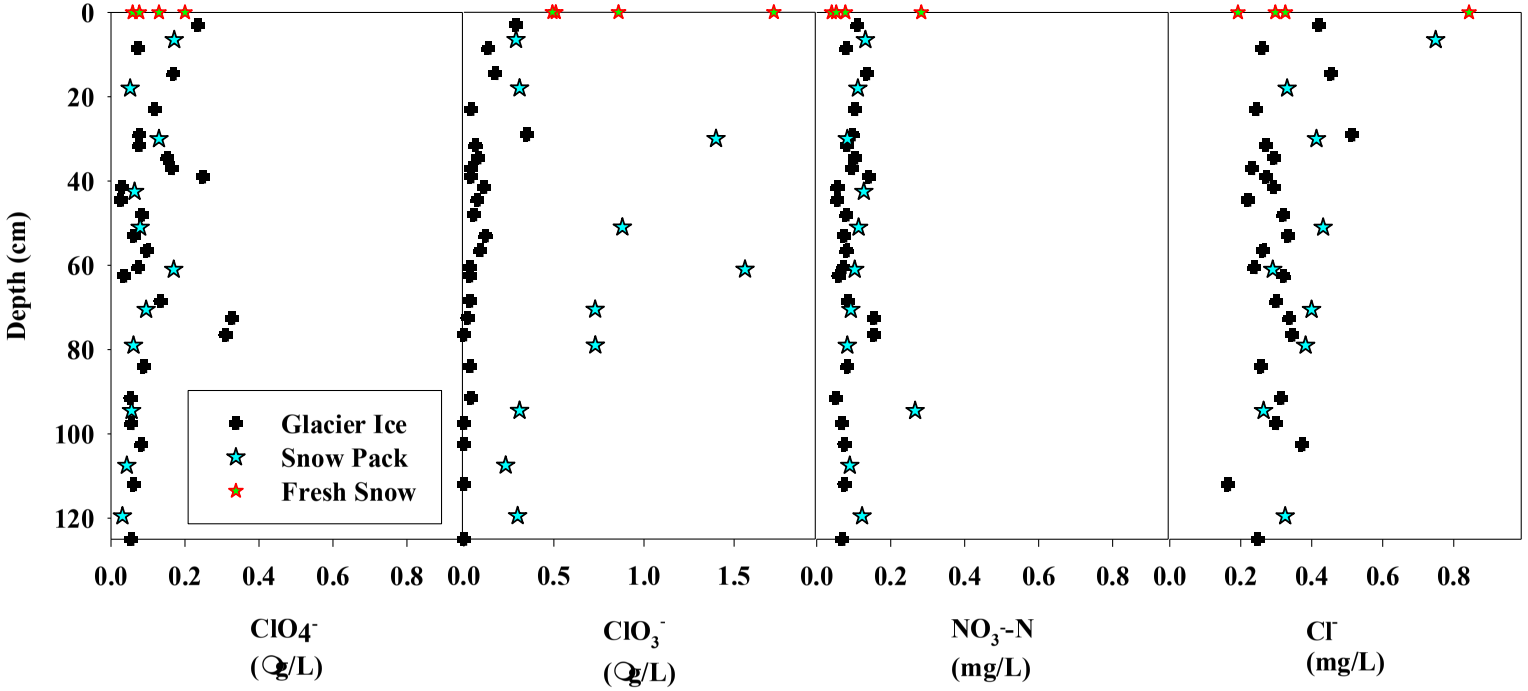

Figure 3. Depth profiles of anion concentrations in glacier ice, snow pack, and fresh snow from University Valley.

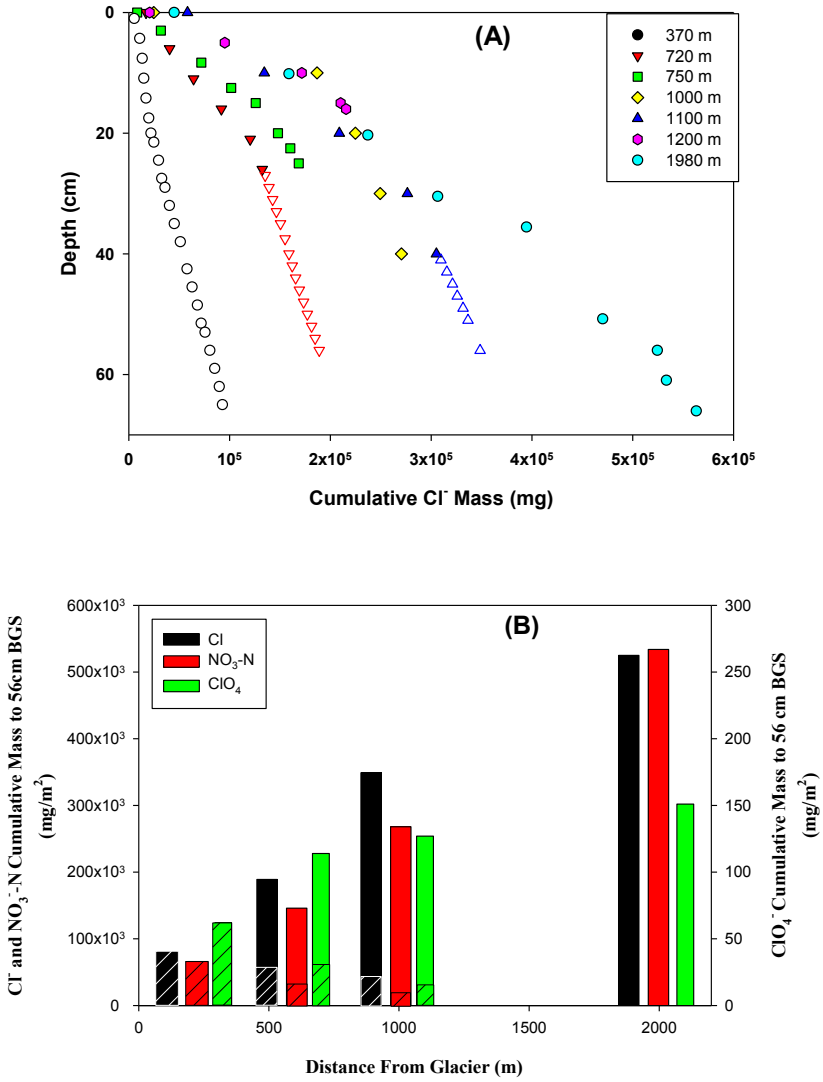

Figure 4. A) Cumulative Cl mass with depth in University Valley soils at various distances downgradient from University Glacier. Filled symbols indicate values in dry cryotic soil an open symbols indicate values in ice-cemented soil. B) Variation in Cl^-, NO_3^--N, and ClO_4^- r per area with distance from glacier. Hatched box represents the mass attributable to ice cem soil below dry cryotic soil. Mass is the cumulative mass to 56cm, the maximum common de

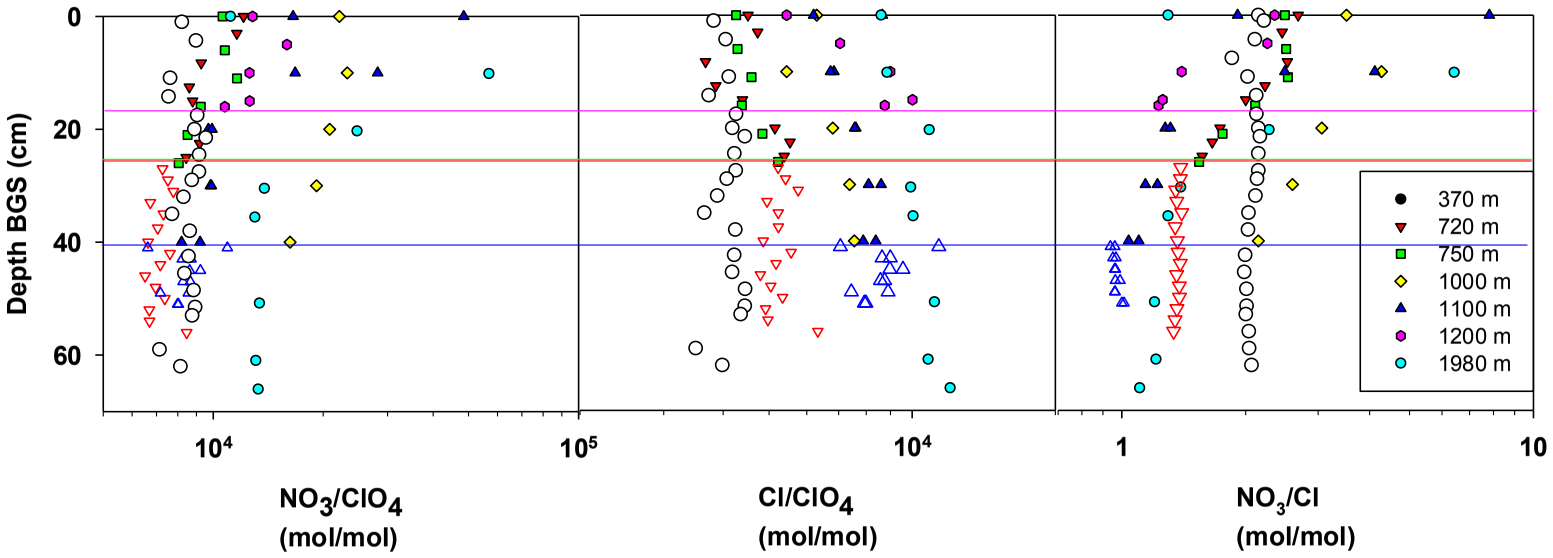

Figure 5. Depth profiles of NO_3/ClO_4, Cl/ClO_4, and NO_3/Cl molar ratios at various distances downgradient from University Glacier when sampled in 2010. Filled symbols indicate values in dry cryotic soil and open symbols indicate values in ice-cemented soil. Horizontal lines indicate the depth to the top of ice-cemented soil (ice table) where known.

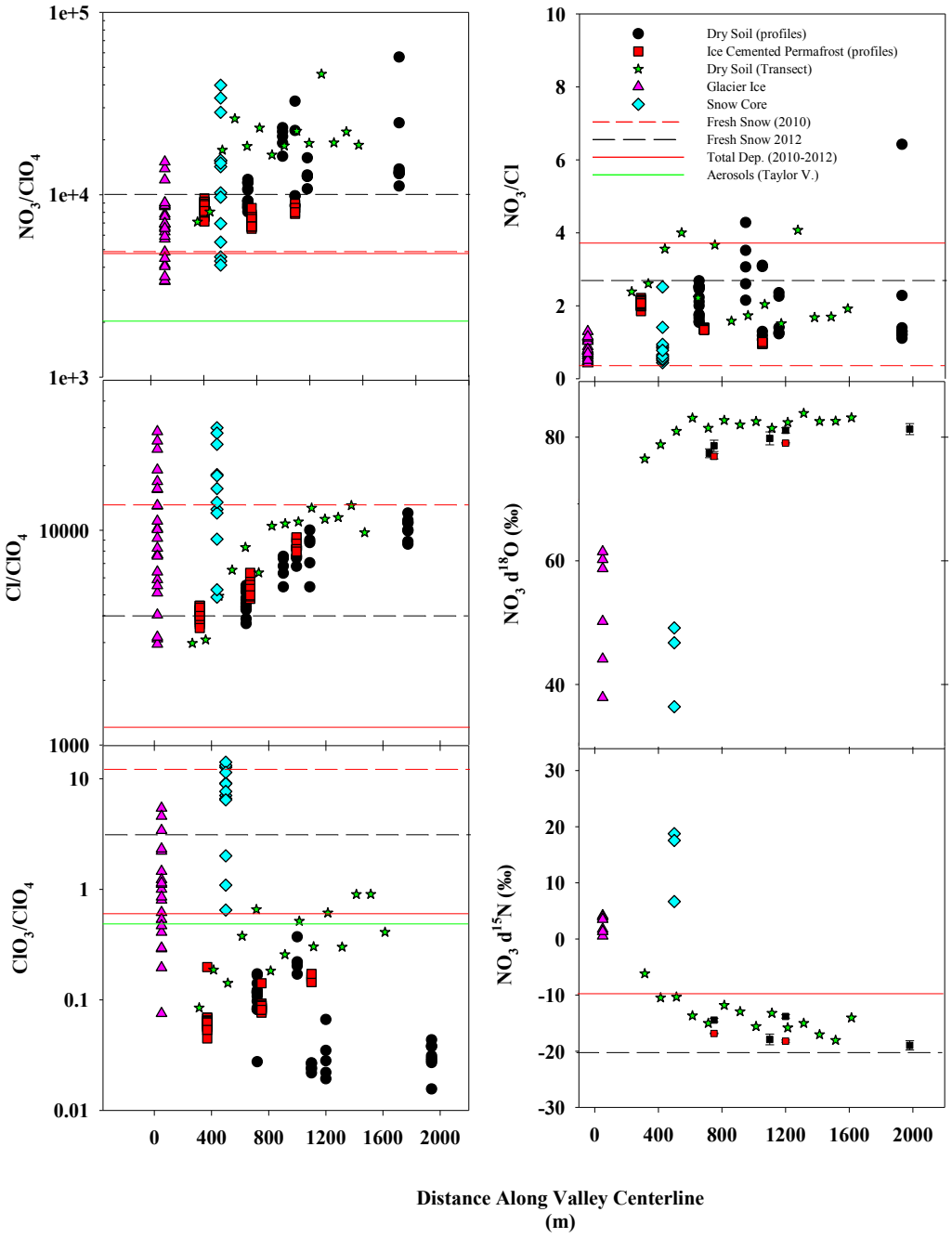

Figure 6. Variation of anion molar ratios and NO_3^- stable isotopic composition in snow, ice, soils with distance from University Glacier. Horizontal lines indicate mean values in aerosc and deposition samples. Aerosols collected from Taylor Valley (2013).

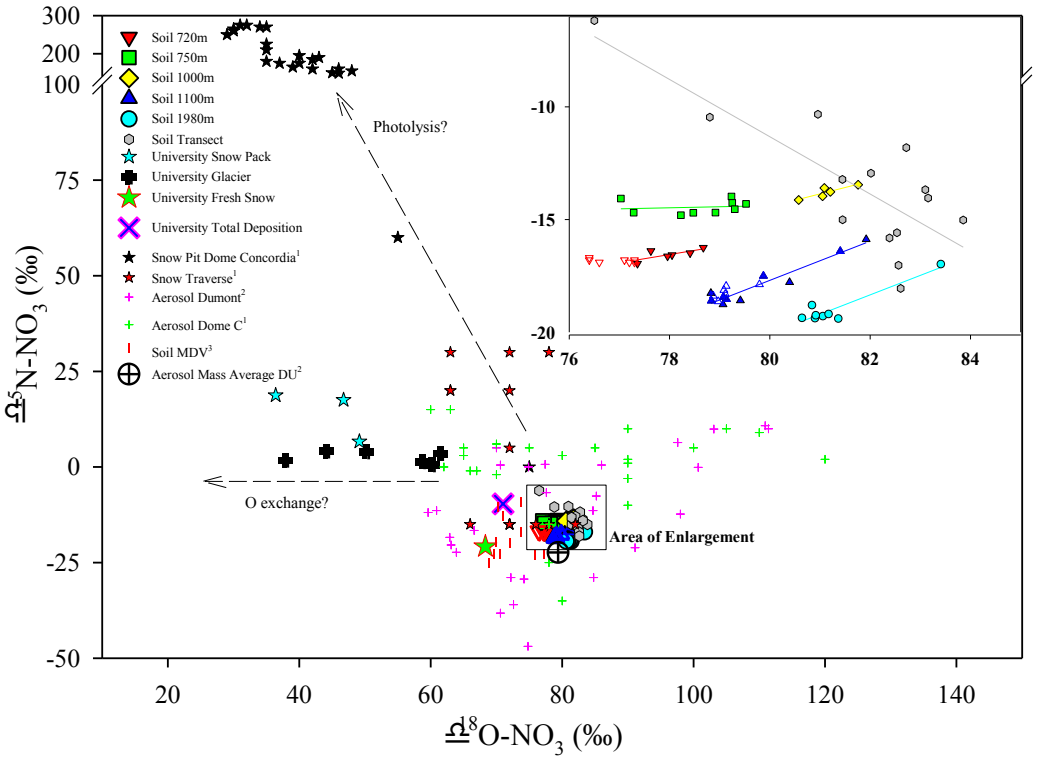

Figure 7. Variation of NO_3^- stable isotopic composition in soil profiles, transect soil samples, snow pack, glacier ice, fresh snow, and total deposition from University Valley. Also shown are previously reported data for MDV soils (Michalski et al., 2005), snow samples including pit and traverse samples from Dome C to Dumont d'Urville (Frey et al., 2009), and aerosol measurements (Savarino et al., 2007). Aerosol mass average values were calculated from one year of data (n=27) at Dumont d'Urville (Savarino et al., 2007). Dashed arrows indicate qualitative directional changes that could be caused by photo-decomposition and oxygen exchange with water. The inset figure gives an enlarged view of variations in University Valley soils; colored lines indicate regressions for subsets of the data and open symbols represent ice cemented permafrost below dry soil. References in legend are: [1] (Frey et al., 2009), [2](Savarino et al., 2007), [3] (Michalski et al., 2005)

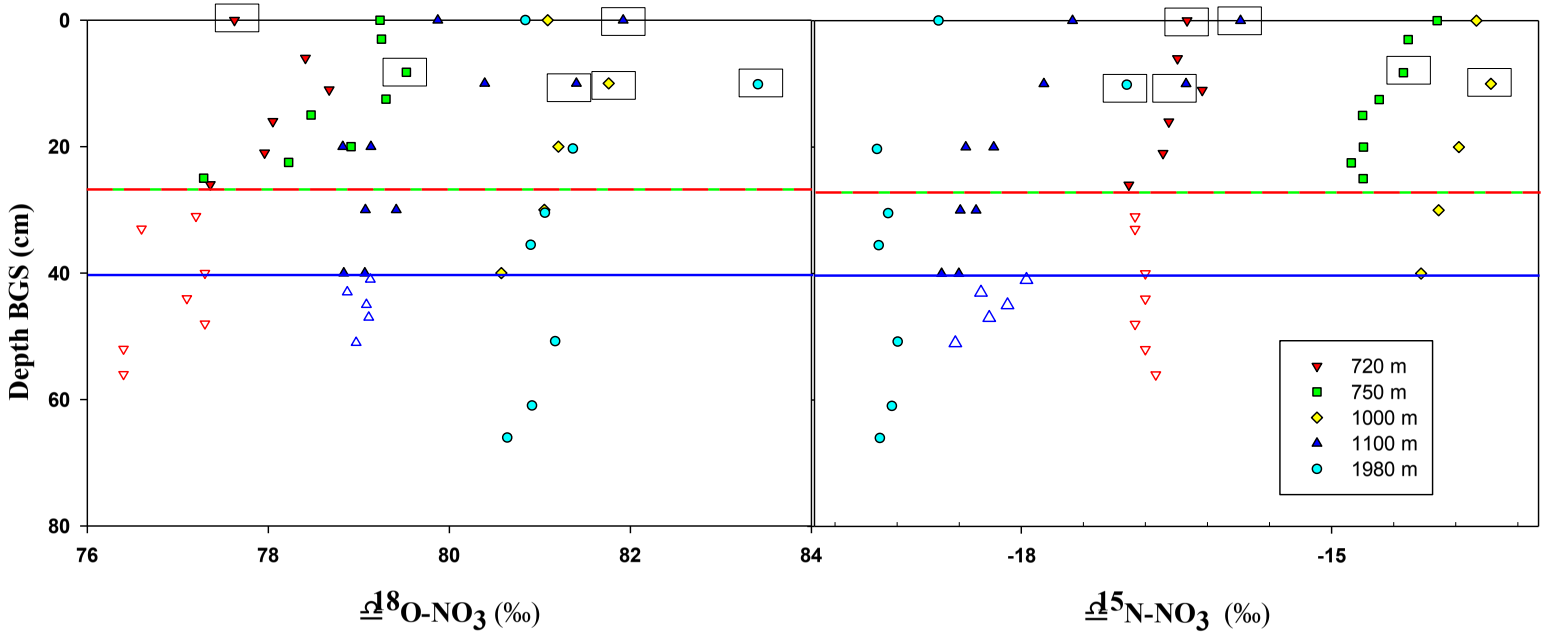

Figure 8. Variation in NO_3 stable isotope composition in University Valley soils at various distances down gradient from University Glacier. Filled symbols indicate values in dry cryotic soil and open symbols indicate values in ice-cemented soil. Boxes indicate maximum NO_3^- concentration for each profile. Horizontal lines indicate the depth to the top of ice-cemented soil (ice table).

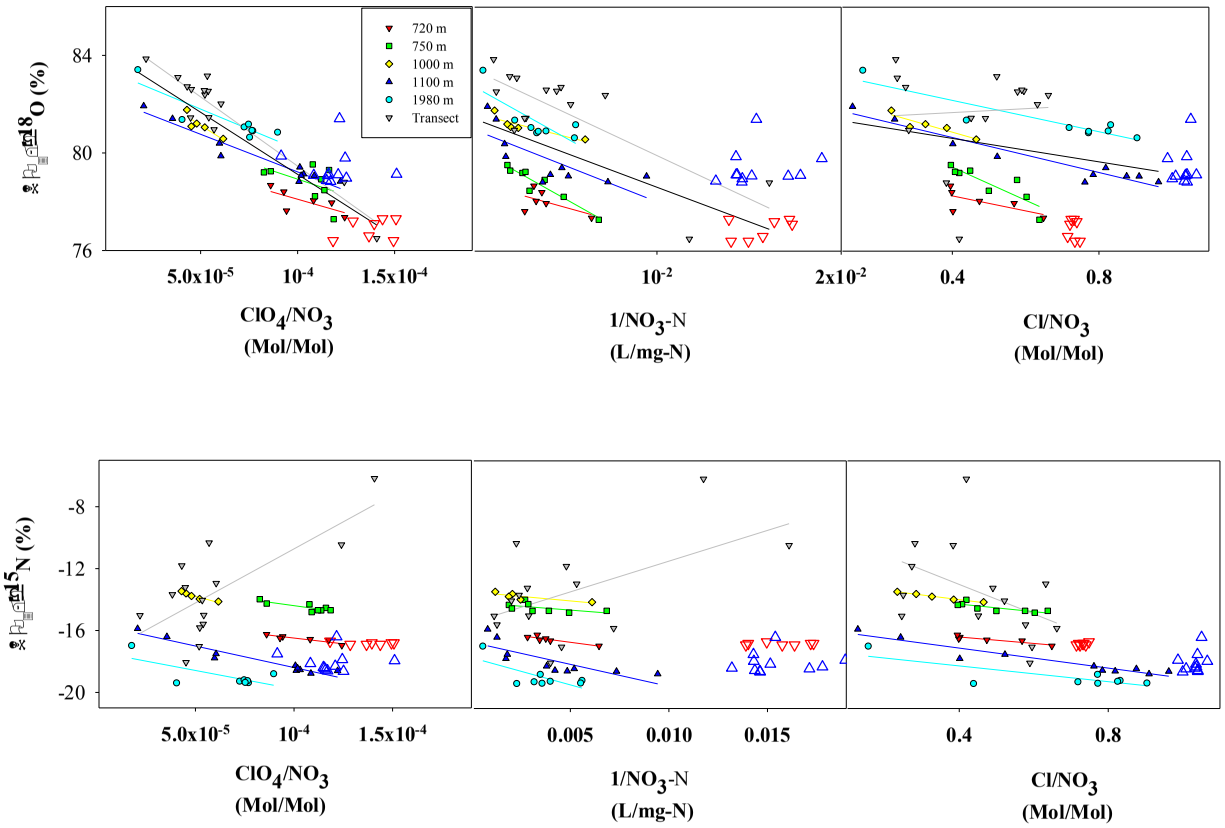

Figure 9. Relationship between $\delta^{18}O$ and $\delta^{15}N$ of NO_3 with NO_3 abundance as reflected by NO_3-N concentration ($1/NO_3$) and molar ratios of ClO_4/NO_3 and Cl/NO_3. Colored lines reflect regression plots for similar colored data points. Open circles represent values of ice cemented soil below dry cryotic soil and are not included in regression analysis. The black line depicts the overall regression plot for all data excluding open symbols in plot.

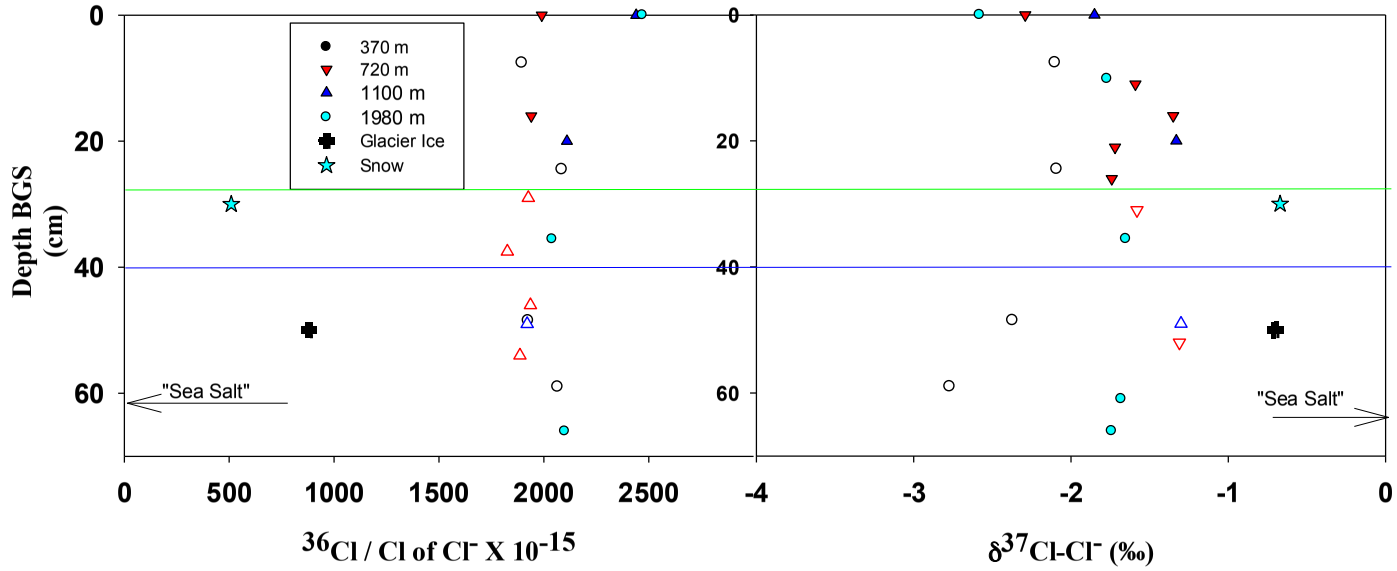

Figure 10. Variation of $^{36}Cl/Cl$ and $\delta^{37}Cl$ values in soil Cl^- with respect to depth and location in University Valley. Filled symbols indicate values in dry cryotic soil and open symbols indicate values in ice-cemented soil. Composite values for snow pack and glacier ice are also shown. Horizontal lines indicate the depth to the top of ice-cemented soil (ice table).

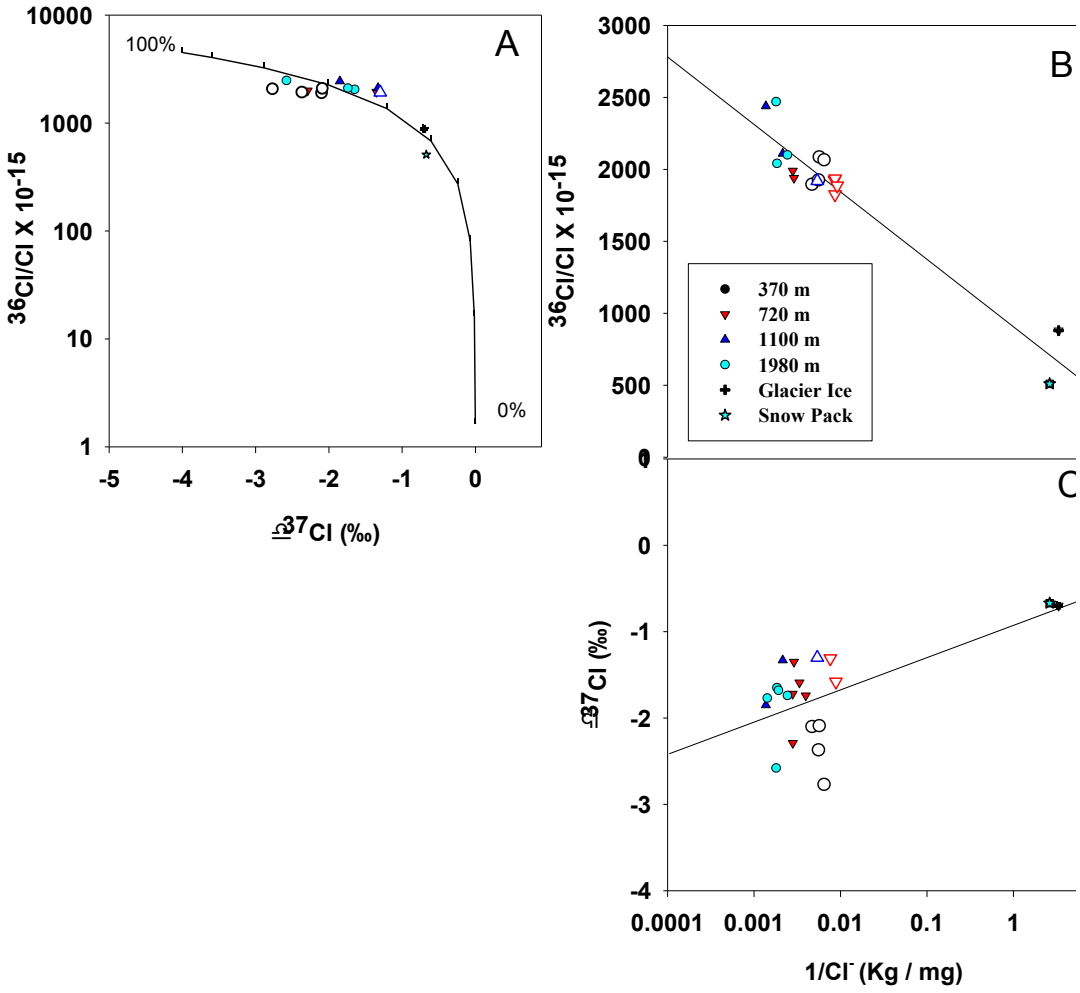

Figure 11. A) Variation in $^{36}Cl/Cl$ ratio with respect to $\delta^{37}Cl$ of samples in University Valley
Filled symbols indicate values in dry cryotic soil and open symbols indicate values in ice-
cemented soil. The curve represents a hypothetical mixing model between stratospheric and
tropospheric components (see text for endmember values). Fractions of the stratospheric
component (high 36Cl/Cl, low $\delta^{37}Cl$) are indicated with tick marks. B) Variation in 36Cl/C
C) $\delta^{37}Cl$ with respect to Cl abundance ($1/Cl^-$). Black lines represent regression line.

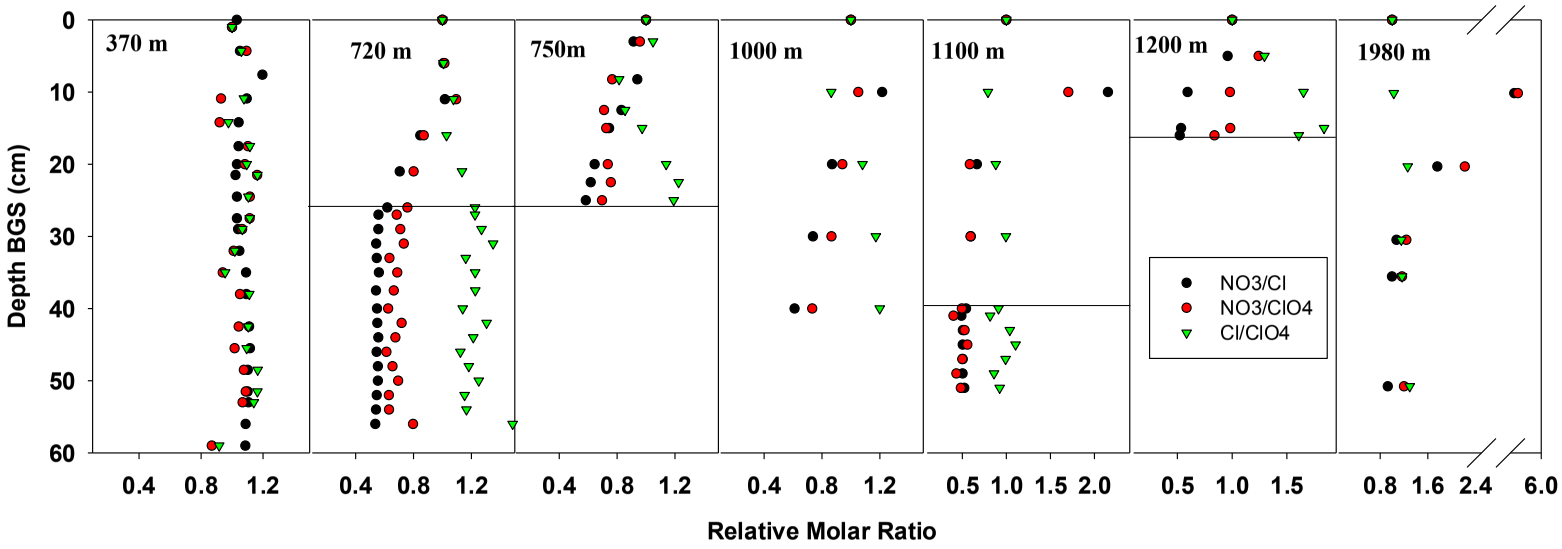

Figure S1. Relative ratios of NO3 and Cl to ClO4 and NO3 to Cl in depth profiles. Ratios (Figure 2) were arbitrarily normalized to the surface ratio to better illustrate relative changes with depth. Horizontal black lines demark interface of ice cemented soil.

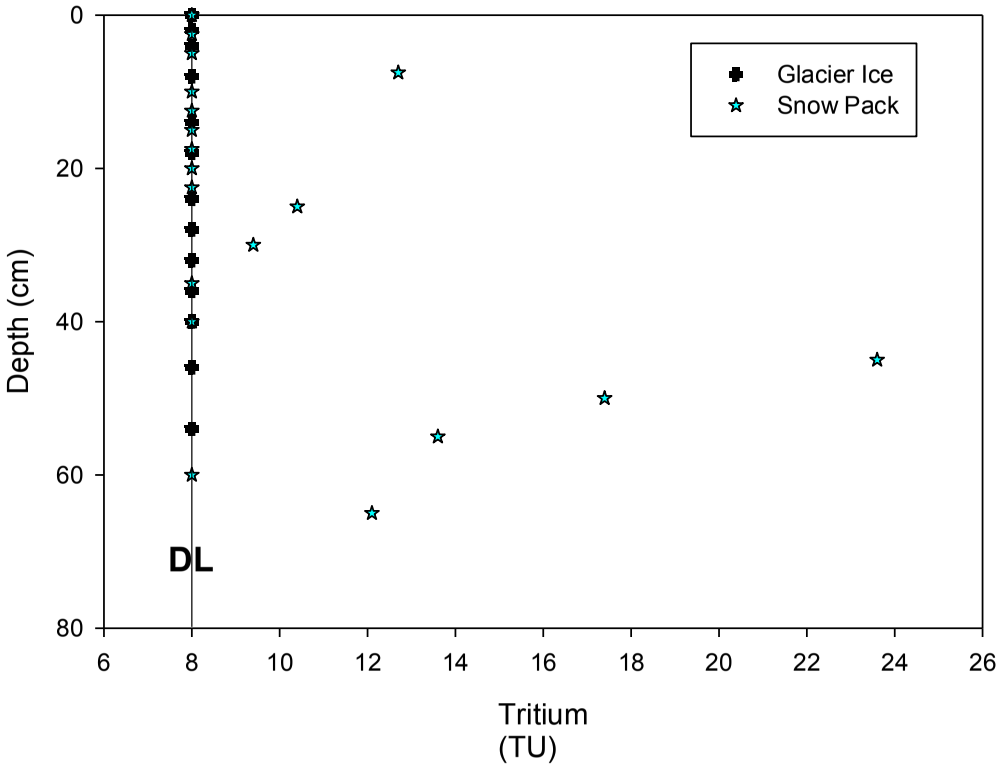

Figure S2. Tritium profiles for the University Valley Glacier and snow pack. Solid line represents the detection limit (8TU). Data is derived from independent cores than those used to determine concentrations of anions.